Department of Geology
University of Cincinnati
P.O. Box 210013
Cincinnati, OH 45221-0013

500 Geology/Physics Building
Phone (513) 556-4195
Fax (513) 556-6931
e-mail: thomas.algeo@uc.edu

January 25th, 2015

Dr. Caroline Slomp
Associate Editor
Biogeosciences

Dear Dr. Slomp:

We have carefully considered the two reviews of the manuscript "Reconstruction of secular variation in seawater sulfate concentrations" and have responded in detail. We have modified our manuscript, where appropriate, per the reviewers' comments. We are forwarding a response letter to the reviews, a marked-up version of the revised manuscript, and a clean version of the revised manuscript for publication in *Biogeosciences*.

The significance of our study is that it develops two quantitative methods for reconstructing ancient seawater sulfate concentrations. One method is based on observed rates of seawater sulfate $\delta^{34}S$ variation ("rate method") and the other on an empirical fractionation trend for microbial sulfate reduction ("MSR-trend method"). We apply these methods to analysis of (1) long-term variation in seawater sulfate concentrations since 635 Ma, and (2) selected intervals of inferred high-frequency seawater sulfate variation in the late Neoproterozoic, Cambrian, Jurassic and Cretaceous.

The two reviews raised some interesting issues, which we are pleased to have an opportunity to address. We have added an extended discussion of the three most important issues as Appendix B of the manuscript. We did not incorporate these issues into the main text, other than as brief summaries with references to Appendix B, because they would have been digressions from the main narrative. We have also responded to all minor comments of the reviewers, making changes to the main text as needed.

This manuscript has not been published previously in any form (except as a Biogeosciences Discussions paper). The submission of this manuscript has been approved by all co-authors.

Sincerely,

Thomas J. Algeo

Professor of Geology

Comments by U.G. Wortmann

General Comments

I have read the paper by Algeo et al with great interest. The authors discuss ways to derive the concentration of sulfate in seawater from the stable isotope ratios observed in sulfides and sulfates. Attempts to do this date back decades, and it is commonly believed that the seawater sulfate concentration varied considerably through time. However, data (as opposed to interpretations) is restricted to a few Cenozoic samples. Some fluid inclusion data exists for the Mesozoic, but it is no longer primary data as their interpretation relies on un-testable assumptions about the chemical composition of Mesozoic seawater.

Response: We thank Dr. Wortmann for a constructive review, in which a number of important issues were raised.

The authors present two different approaches to estimate the marine sulfate concentration. The first one is based on the rate of change of the observed S-isotope ratio, and basically states that if we assume that modern burial/weathering fluxes are representative, the rate of change is a measure of the reservoir size (aka sulfate concentration). As far as I understand it, this approach is only valid if the rate of change is equal to the residence time of the respective system. The authors allude to this somewhat obliquely on page 13192, line 8ff. However, what happens if the fluxes become so big that the rate of change is considerably faster then the residence time, and even affect the reservoir size itself?

Response: First, the mathematical relationships underlying the rate method deserve clarification. The reviewer's comment above, taken literally, is incorrect. Rate of change has units of per mille per million years (‰ Myr^{-1}) and therefore cannot be "equal to" residence time, which has units of Myr^{-1}. We infer the reviewer's intended meaning to be that the maximum possible rate of change in seawater sulfate $\delta^{34}S$ (i.e., $\partial\delta^{34}S_{SO4}/\partial t(max)$) is inversely proportional to residence time (τ):

$$\partial\delta^{34}S_{SO4}/\partial t(max) \equiv \tau^{-1} \qquad [\text{or } \tau \equiv \partial\delta^{34}S_{SO4}/\partial t(max)^{-1}] \qquad (B0)$$

The exact quantitative form of this relationship can be derived from Equation 2 of Algeo et al. (2014), reorganization of which yields:

$$M_{SW} / F_{PY} = k_1 \times \Delta^{34}S_{CAS\text{-}PY} / \partial\delta^{34}S_{CAS}/\partial t(max) \qquad (B1)$$

[Note that here and in subsequent equations, M_{SW} is 1.3×10^{21} g, F_{PY} has units of g yr^{-1}, $\Delta^{34}S_{CAS\text{-}PY}$ has units of per mille (‰), $\partial\delta^{34}S_{CAS}/\partial t(max)$ has units of ‰ Myr^{-1}, τ has units of yr, and k_1 and k_2 are constants equal to 10^6 (no units) and 2.22×10^{-20} mM g^{-1}, respectively (see Algeo et al., 2014, for further explanation).] The residence time of sulfur in seawater is equal to the mass of seawater sulfate divided by the total sink flux, i.e., the reduced sulfur flux (F_{PY}) plus the oxidized sulfur flux (F_{EVAP}):

$$\tau = M_{SW} / (F_{PY} + F_{EVAP}) \quad \text{(B2)}$$

Letting ϕ_{PY} be the fraction of the total S flux represented by pyrite burial (i.e., $F_{PY} / (F_{PY} + F_{EVAP})$), then:

$$\tau \times \phi_{PY}^{-1} = M_{SW} / F_{PY} \quad \text{(B3)}$$

And substitution into Equation B1 yields:

$$\tau \times \phi_{PY}^{-1} = k_1 \times \Delta^{34}S_{CAS\text{-}PY} / \partial\delta^{34}S_{CAS}/\partial t(max) \quad \text{(B4)}$$

Equation A5 thus quantifies the inverse proportionality between the maximum rate of change of seawater sulfate $\delta^{34}S$ and the residence time of sulfur in seawater (cf. Eq. B0).

Second, the reviewer opines that "this approach is only valid if the rate of change is equal to the residence time of the respective system." We agree that the rate method yields an accurate estimate of seawater sulfate concentrations only if F_{PY} is parameterized in a manner consistent with τ, which basically requires the system to be in equilibrium. If a value for F_{PY} is chosen that is much larger or smaller than the true equilibrium flux, then seawater sulfate concentrations will be overestimated or underestimated, respectively. We consider these issues further in our reply to the next comment.

Action: We have added a brief mention of these issues to the text of the manuscript and an extended discussion as Appendix B of the revised manuscript. We did not insert this material into the text as it is of tangential importance to the development of the main theme of our paper.

This brings me to my main concern with this model. Equation 3 relates the rate of change to the marine sulfate concentration using a time invariant pyrite burial flux. However, the pyrite burial flux itself depends on the marine sulfate concentration. This dependency is weak above 12mM, but becomes significant for lower concentrations. While the exact relation is not known, and probably changes through time, Wortmann and Chernyavsky (2007) provide a useable parametrization in their supplemental data. This point requires attention before the MS can be published.

Response: The reviewer has raised an excellent point. We agree that the pyrite burial flux has almost certainly varied through time. Since pyrite burial flux is a component of Equations 2 and 3, variations in this parameter will influence calculated seawater sulfate concentrations. Thus, it would be desirable to parameterize such variation in our rate method.

First, we explored the effects of varying pyrite burial fluxes on seawater sulfate estimates as follows. Equations 2-3 of Algeo et al. (2014) have four variables: $[SO_4^{2-}]_{SW}$ (or M_{SW}, since these

are inter-convertible via Equation 4), F_{PY}, $\Delta^{34}S_{CAS\text{-}PY}$, and $\partial\delta^{34}S_{SO4}/\partial t$. However, $\Delta^{34}S_{CAS\text{-}PY}$ can be modeled as a function of $[SO_4^{2-}]_{SW}$ (i.e., the MSR trend of Figure 2 and Equation 6), reducing the number of potentially independent variables to three (we state "potentially independent" as there may in fact be some dependency among these variables). Now it is possible to explore the effects of simultaneous variations in $[SO_4^{2-}]_{SW}$ and F_{PY} on $\partial\delta^{34}S_{SO4}/\partial t$(max) via a modified form of Equation 2:

$$\partial\delta^{34}S_{CAS}/\partial t(max) = k_1 \times k_2 \times F_{PY} \times \exp(\log[SO_4^{2-}]_{SW} * 0.42 + 1.10) / [SO_4^{2-}]_{SW} \qquad (B5)$$

The three modeled parameters exhibit log-linear relationships, with larger $\partial\delta^{34}S_{CAS}/\partial t$(max) associated with larger $[SO_4^{2-}]_{SW}$ and F_{PY} (Fig. B1). $\partial\delta^{34}S_{CAS}/\partial t$(max) scales linearly with F_{PY}, so uncertainty in the latter parameter is directly mirrored in the former parameter. In our study (Algeo et al., 2014), we used fixed estimates of F_{PY}, either 4×10^{13} g yr^{-1} for oxic oceans or 10×10^{13} g yr^{-1} for anoxic oceans. This range of F_{PY} values is consistent with variation in $\partial\delta^{34}S_{CAS}/\partial t$(max) from ~1 to 100 ‰ Myr^{-1} (Fig. B1). Wortmann and Chernyavsky (2007) inferred $[SO_4^{2-}]_{SW}$-dependency of the pyrite burial flux (their figure 4; red curve, Fig. B1). If correct, this relationship indicates that variation in $\partial\delta^{34}S_{CAS}/\partial t$(max) cannot exceed ~3 ‰ Myr^{-1} under any set of conditions. This result is at odds with numerous well-documented examples of higher rates of $\delta^{34}S_{CAS}$ variation in paleomarine sedimentary units (e.g., Algeo et al., 2014, Table A4).

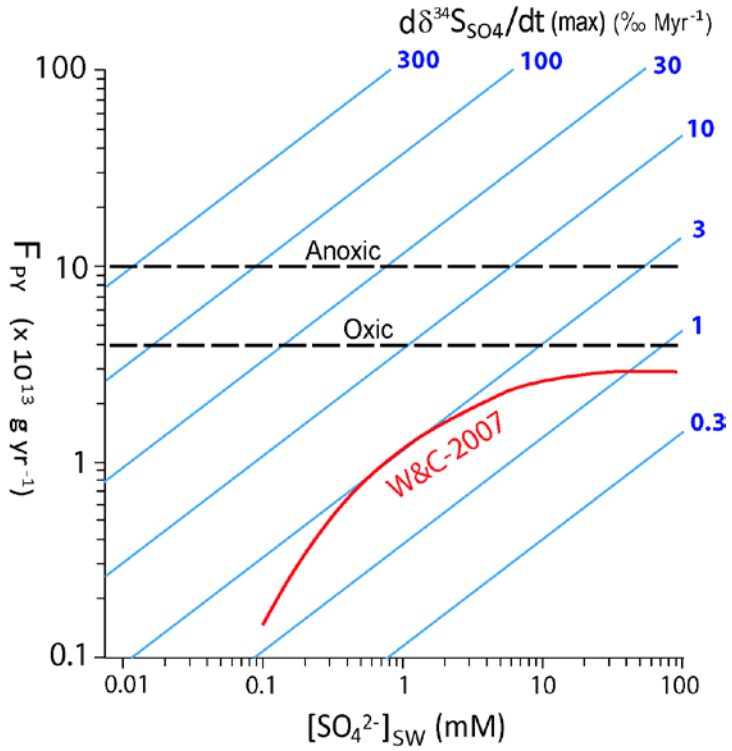

Figure B1

Figure B1. Relationship of $\partial\delta^{34}S_{CAS}/\partial t$(max) to F_{PY} and $[SO_4^{2-}]_{SW}$, with $\Delta^{34}S_{CAS\text{-}PY}$ estimated as a function of $[SO_4^{2-}]_{SW}$ (Figure 2, Equation 6 of Algeo et al., 2014). The dashed horizontal lines represent the pyrite burial fluxes used by Algeo et al. (2014) for anoxic and oxic paleomarine systems. The red line represents the $[SO_4^{2-}]_{SW}$-dependency of the pyrite burial flux as given in figure 4 of Wortmann and Chernyavsky (W&C-2007). Note that according to the latter relationship, $\partial\delta^{34}S_{CAS}/\partial t$(max) values cannot exceed ~3 ‰ Myr^{-1} under any set of conditions.

As noted by the reviewer, variable pyrite burial fluxes will certainly have an influence on seawater sulfate concentration estimates. We have tested this influence by applying the relationship between $[SO_4^{2-}]_{SW}$ and F_{PY} given by Wortmann and Chernyavsky (2007, their figure 4) to our rate-method calculations. Their relationship can be reduced to a logarithmic expression:

$$F_{PY} = 0.7681 \times \ln([SO_4^{2-}]_{SW}) + 1.405 \quad \text{(B6)}$$

where F_{PY} is in units of 10^{13} g yr^{-1} (rather than in mol yr^{-1}, as in their paper) and $[SO_4^{2-}]_{SW}$ is in units of mM. This expression yielded a r^2 of 0.98 in relation to Wortmann and Chernyavsky's curve (their figure 4). In making use of temporally variable pyrite burial fluxes for calculation of seawater sulfate estimates, Equations 3 and 4 of our paper (Algeo et al., 2014) must be reorganized as follows:

$$[SO_4^{2-}]_{SW}(max) / F_{PY} = k_1 \times k_2 \times \Delta^{34}S_{CAS\text{-}PY} / \partial\delta^{34}S_{CAS}/\partial t(max) \quad \text{(B7)}$$

Although Equation B7 has two unknowns, i.e., $[SO_4^{2-}]_{SW}(max)$ and F_{PY}, it can be solved because F_{PY} is a function of $[SO_4^{2-}]_{SW}$ in figure 4 of Wortmann and Chernyavsky (2007). The empirical relationship between $[SO_4^{2-}]_{SW}$ and $[SO_4^{2-}]_{SW}(max) / F_{PY}$ derived from that figure is given by the polynomial equation:

$$[SO_4^{2-}]_{SW}(max) / F_{PY} = -0.0018([SO_4^{2-}]_{SW})^2 + 0.2842([SO_4^{2-}]_{SW}) + 0.4651 \quad \text{(B8)}$$

With substitution and reorganization, Equations B7 and B8 yield:

$$0 = -0.0018([SO_4^{2-}]_{SW})^2 + 0.2842([SO_4^{2-}]_{SW}) + (0.4651 - k_1 \times k_2 \times \Delta^{34}S_{CAS\text{-}PY}/[\partial\delta^{34}S_{CAS}/\partial t(max)]) \quad \text{(B9)}$$

This second-order polynomial equation can now be solved for $[SO_4^{2-}]_{SW}$ using the quadratic solution, after which F_{PY} can be calculated from Equation B6.

Using Equation B9, we calculated $[SO_4^{2-}]_{SW}$ on the basis of $\partial\delta^{34}S_{CAS}/\partial t(max)$ and $\Delta^{34}S_{CAS\text{-}PY}$. These relationships are plotted as variation in $\partial\delta^{34}S_{CAS}/\partial t(max)$ as a function of $[SO_4^{2-}]_{SW}$ and $\Delta^{34}S_{CAS\text{-}PY}$ (Fig. B2; cf. Figure 1 of Algeo et al., 2014). At high $[SO_4^{2-}]_{SW}$, the two sets of $\partial\delta^{34}S_{CAS}/\partial t(max)$ curves are nearly co-linear, which is because the value of F_{PY} in figure 4 of Wortmann and Chernyavsky (2007) for $[SO_4^{2-}]_{SW}$ >10 mM is nearly invariant and similar to the flux that we used (i.e., 4×10^{13} g yr^{-1}). In contrast, the two sets of curves diverge sharply at $[SO_4^{2-}]_{SW}$ <1 mM, which is a consequence of the much lower F_{PY} values associated with low seawater sulfate concentrations in the Wortmann and Chernyavsky curve.

There are a couple of worthwhile observations to make about the $\partial\delta^{34}S_{CAS}/\partial t(max)$ curves based on the Wortmann and Chernyavsky (2007) relationship. First, the MSR trend of Algeo et

al. (2014) corresponds almost entirely to a limited range of $\partial\delta^{34}S_{CAS}/\partial t(max)$ values (i.e., 2 to 4; Fig. B2). This suggests that there ought to be quite limited variation in $\partial\delta^{34}S_{CAS}/\partial t(max)$ over a wide range of seawater sulfate concentrations in nature. Second, many combinations of the two sediment parameters that can be measured (i.e., $\Delta^{34}S_{CAS\text{-}PY}$ and $\partial\delta^{34}S_{CAS}/\partial t(max)$) cannot yield a $[SO_4^{2-}]_{SW}$ estimate. For example, for a $\Delta^{34}S_{CAS\text{-}PY}$ value of 7‰, any $\partial\delta^{34}S_{CAS}/\partial t(max)$ value >4 does not yield an estimate of $[SO_4^{2-}]_{SW}$ (Fig. B2). This situation exists because high rates of variation in seawater sulfate $\delta^{34}S$ are not possible where the pyrite burial flux is sharply curtailed by $[SO_4^{2-}]_{SW}$-dependency (as in figure 4 of Wortmann and Chernyavsky, 2007). However, many paleomarine units exhibit $\partial\delta^{34}S_{CAS}/\partial t(max)$ values outside the narrow range permitted by the Wortmann and Chernyavsky (2007) relationship (see Table A4 and Figures 6-8 of Algeo et al., 2014).

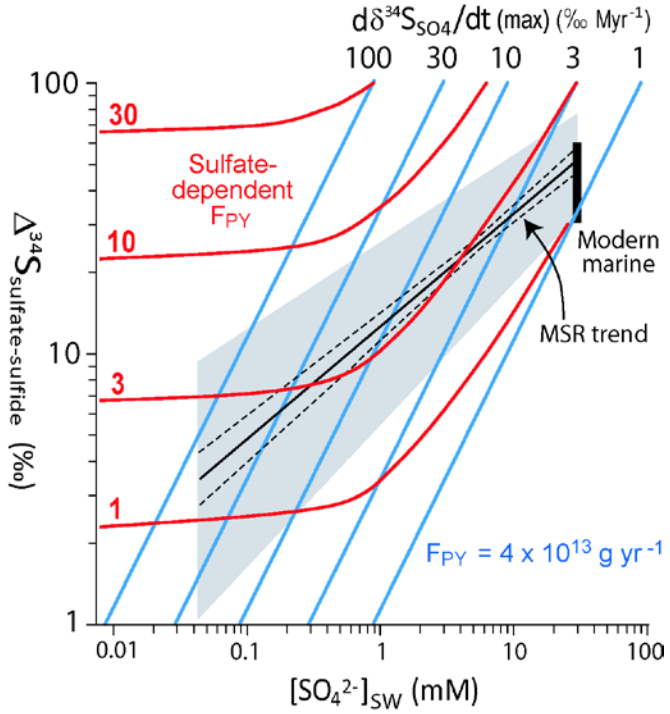

Figure B2

Figure B2. $\partial\delta^{34}S_{CAS}/\partial t(max)$ values calculated using the fixed pyrite burial flux of Algeo et al. (2014) (blue diagonal lines) and the sulfate-dependent pyrite burial fluxes of Wortmann and Chernyavsky (2007; their figure 4) (red curves). Note that, for the latter curves, many combinations of the two measured sediment parameters ($\Delta^{34}S_{CAS\text{-}PY}$ and $\partial\delta^{34}S_{CAS}/\partial t(max)$) cannot yield a $[SO_4^{2-}]_{SW}$ estimate. Shown for reference is the MSR trend of Algeo et al. (2014).

What conclusions can be reached from this analysis? Use of $[SO_4^{2-}]_{SW}$-dependent values of F_{PY} allows no $\partial\delta^{34}S_{CAS}/\partial t(max)$ values greater than ~3 ‰ Myr^{-1} under any set of conditions, which is at odds with the results of numerous published studies. If the Wortmann and Chernyavsky (2007) parameterization of the F_{PY}-$[SO_4^{2-}]_{SW}$ relationship is correct, then one must conclude either that all of these published higher rates are products of uncertain geochronologic dating, diagenetic artifacts, or sample processing and analytical problems. This seems inherently unlikely. On the other hand, use of fixed values for F_{PY} in the rate-method calculations of Algeo et al. (2014) yields estimates of $[SO_4^{2-}]_{SW}$ that are—for the most part—consistent with estimates of $[SO_4^{2-}]_{SW}$ based on the MSR-trend method (see Figures 6-8 of Algeo et al., 2014, for examples). The consistency of results for these two quasi-independent methods thus

provides a degree of confidence in their validity. Does this mean perforce that pyrite burial fluxes are not dependent on seawater sulfate concentrations? Not necessarily—some form of $[SO_4^{2-}]_{SW}$-dependency may exist, but perhaps the form of this dependency is different from that given in Wortmann and Chernyavsky (2007).

Action: We have added a brief mention of these issues to the text of the manuscript and an extended discussion as Appendix B of the revised manuscript. We did not insert this material into the text as it is of tangential importance to the development of the main theme of our paper.

We also calculated paleoseawater sulfate concentrations using $[SO_4^{2-}]_{SW}$-dependent pyrite burial fluxes. For the rate-method estimates of Phanerozoic $[SO_4^{2-}]_{SW}$ given in Figure 4 and Table A3 of Algeo et al. (2014), this procedure yields $[SO_4^{2-}]_{SW}$ estimates that are close to (±10%) our original values. This result was obtained because the $\partial\delta^{34}S_{CAS}/\partial t(max)$ values of the Phanerozoic record are almost uniformly low (<3 ‰ Myr^{-1}; Figure 3b of Algeo et al., 2014), which is mainly a consequence of data smoothing in constructing the Phanerozoic curve (see discussion in Algeo et al., 2014). At such low $\partial\delta^{34}S_{CAS}/\partial t(max)$ values, there is little difference in the $[SO_4^{2-}]_{SW}$ estimates generated with and without $[SO_4^{2-}]_{SW}$-dependent pyrite burial fluxes (see Fig. B2). For the intervals of high-frequency $\delta^{34}S_{CAS}$ variation shown in Figures 6-8 and Table A4 of Algeo et al. (2014), many units have combinations of $\Delta^{34}S_{CAS\text{-}PY}$ and $\partial\delta^{34}S_{CAS}/\partial t(max)$ values that cannot yield an estimate of $[SO_4^{2-}]_{SW}$ per the Wortmann and Chernyavsky (2007) relationship.

In their second approach, the authors provide an empirical relationship between sulfate concentration and the difference between the S-isotope ratios measured from sulfate and pyrite. This is intriguing but it remains unclear to me how reliable this proxy is, because we have not enough data to check their results against (Fig. 5 insinuates to much here, as the majority of the data shown there is not primary, but proxy data). I am particularly concerned about the mismatch between the authors data and the reconstructions by Wortmann and Paytan (2012). Granted, the latter paper is controversial, however the Cretaceous to Eocene interval is the one time in Earth history where we have large and fast S-isotope variations, a highly resolved marine S-isotope record, and fluid inclusion data which suggest sulfate concentration changes on the order of 20 mM. So this requires special attention.

Response: The first point relates to whether mineral sulfide $\delta^{34}S$ is an adequate proxy for aqueous sulfide $\delta^{34}S$ in developing the MSR trend (Figure 2 of Algeo et al., 2014). We have already addressed this point at length in our paper (see second paragraph of Section 2.2), considering S-isotopic fractionations between aqueous sulfide and mineral sulfide. One point that bears reflection is that estimates of paleoseawater $[SO_4^{2-}]_{SW}$ are based not on aqueous sulfide $\delta^{34}S$, which cannot be measured for paleomarine systems, but on mineral sulfide (generally pyrite) $\delta^{34}S$. Therefore, the critical relationship for establishing a viable MSR-trend proxy for $[SO_4^{2-}]_{SW}$ is that between sulfate $\delta^{34}S$ and mineral sulfide $\delta^{34}S$.

The second point claims a mismatch between our data and that of Wortmann and Paytan (2012). We presume that the reviewer is referring to the differences in $[SO_4^{2-}]_{SW}$ estimates for the ~120 to 50 Ma interval, during which the estimates of Wortmann and Paytan (2012) are uniformly <7 mM (their figure 2b) whereas those of Algeo et al. (2014) are ~13-16 mM (with an uncertainty range of ca. 2X; Figure 4). We agree that there are modest differences in absolute $[SO_4^{2-}]_{SW}$ estimates between these records, although the 120-50-Ma interval is one of low seawater sulfate concentrations (relative to the preceding and following intervals) in both studies, so there is significant agreement in that regard. The absolute values of the Phanerozoic $[SO_4^{2-}]_{SW}$ curve in Figure 4 of Algeo et al. (2014) are a function of the input dataset, which is the Phanerozoic $\Delta^{34}S_{CAS\text{-}PY}$ record of Wu et al. (2010). The latter is a large compilative dataset that perforce entailed considerable data averaging, which is likely to have dampened the range of variation in the long-term trend. If so, it is possible that the lower $[SO_4^{2-}]_{SW}$ estimates for the 120-50-Ma interval of Wortmann and Paytan (2012) are more accurate. However, the fact that we have used a somewhat smoothed input dataset in calculating a Phanerozoic $[SO_4^{2-}]_{SW}$ curve does not comment in any way on the validity of the $\Delta^{34}S_{CAS\text{-}PY}$-$[SO_4^{2-}]_{SW}$ relationship (i.e., the MSR trend) in our paper (Algeo et al., 2014, Figure 2).

Action: We have added a brief discussion of these issues to the revised manuscript.

If I understand the authors correctly, they argue: A) that the current $\delta^{34}S$ record could be a local record in the Tethys basin. However a significant part of the Cretaceous $\delta^{34}S$ data is from Site 305 (Shatsky Rise, W-Pacific) and fits nicely with the data from Site 766 (Indian Ocean, possibly restricted); B) that their model may not capture short term draw down events. If so, two questions come to mind: A) Even if the draw down may be short term, the recovery will take a very long time. Using modern fluxes, Wortmann and Paytan (2012) estimate that it takes 60 Million years for the sulfate concentration to recover. If the Algeo et al. model is indeed insensitive to "short term" draw down events, short term events will introduce considerable error in their reconstructions. B) More importantly however, why would be a sulfate-pyrite difference model like the one proposed here, be insensitive to short term draw down?

Response: Regarding the possible influence of restricted watermasses, we offered the hypothesis that the unusually low rate-based $[SO_4^{2-}]_{SW}$ estimates of a subset of the Mesozoic units shown in Figure 8 of Algeo et al. (2014) may have been due to watermass restriction. The units in question (labeled *r*, *t*, *t'*, *v*, and *w* in Figure 8) were located in the north-central Tethys (Tibet), western Tethys (England), South Atlantic, and North American Western Interior Seaway. A case can be made for some degree of watermass restriction in each area, although this remains a hypothesis, and it is possible that additional S-isotopic work might upwardly revise the rate-based $[SO_4^{2-}]_{SW}$ estimates for these units. We do not believe that these findings conflict with the results of Wortmann and Paytan (2012).

Regarding the rate of recovery of seawater sulfate concentrations, Wortmann and Paytan (2012) infer a recovery interval of ~60 Myr following a 120-Ma drawdown event. However, the mathematics of reservoir theory shows that recovery intervals should be of similar duration to the residence time of a given seawater component, which is ~13 Myr for seawater sulfate at

present and would be shorter if the recovery "target" concentration were lower. Other factors must have contributed to the extended recovery interval observed by Wortmann and Paytan (2012).

Regarding the insensitivity of our model to short-term seawater sulfate drawdown, this is a function of the input dataset, which is the Phanerozoic $\Delta^{34}S_{CAS\text{-}PY}$ record of Wu et al. (2010), and not of the MSR-trend method of estimating paleoseawater $[SO_4^{2-}]_{SW}$. The Wu et al. record is a large compilative dataset that perforce entailed considerable data averaging, which is likely to have dampened the range of variation in the long-term trend and reduced or eliminated short-term events. The Phanerozoic $[SO_4^{2-}]_{SW}$ curve that we generated from this record (Fig. 4 of Algeo et al., 2014) should be regarded as representative of long-term seawater sulfate trends but without short-term drawdown events. This interpretation is reinforced by comparison of our Phanerozoic $[SO_4^{2-}]_{SW}$ curve with estimates based on other techniques (Fig. 5 of Algeo et al., 2014). The MSR-trend method of estimating paleoseawater $[SO_4^{2-}]_{SW}$ is certainly capable of capturing short-term drawdown events, provided that these events are present in the $\Delta^{34}S_{CAS\text{-}PY}$ record that is used as input data for $[SO_4^{2-}]_{SW}$ calculations.

Action: We have added a brief discussion of these issues to the revised manuscript.

Specific Comments

1. p13188 l10, and p 13192 l10. The rate of change is not only determined by reducing the input/output flows to zero. You could also double or triple those flows, which would have a considerable effect on the rate of change. Or is this an oblique way to state that the model is only valid if the rate of change is equal to the residence time?

Response: This question was fully addressed above.

2. p13188 l20 ff and later in the manuscript. I always thought that the Early Triassic sulfate concentrations are low. The rapid changes observed during this time certainly require sulfate concentrations below 10 mM (e.g. Song et al., 2014)?

Response: We agree, and this point is addressed specifically on p13188 l22-24 and later in the paper.

3. p13188 l23 What is the meaning of "varied only slightly since 250 Ma"? Some of our most reliable data on sulfate concentrations is of Jurassic and Cretaceous age, and even fluid inclusion data suggest pretty dramatic changes from 8 mM during the Early Cretaceous to modern values around 28 mM (Lowenstein et al., 2001, 2003; Demicco et al., 2005).

Response: We cite a range of ~10-30 mM in the same sentence in which we state "varied only slightly since 250 Ma". Variation over a range of ~3× is small compared to the much larger variations (probably ~20-100×) that occurred during the Neoproterozoic and Paleozoic. We

cannot go into complex details in the Abstract; more specific values and ranges are cited later in the paper.

4. p13188 l24 I'd add the Cretaceous here, see above.

Response: OK, done.

5. p 13191 l15 there is a pretty rich literature on the subject, however the paper cited here only discusses data from a lake and lagoon.

Response: Agreed. We have added additional citations.

6. p p 13192 eq 2 Fpyr itself depends on the sulfate concentration (Wortmann and Chernyavsky, 2007). As stated, the equation will only work for concentrations above 12 mM.

Response: This question was fully addressed above.

7. p13193 l20. I seem to remember that the Paytan et al. (1998) data showed faster variations?

Response: In Figure 1a of the Paytan et al. (1998) paper, the intervals of most rapid variation in seawater sulfate are (1) from ~18.0‰ to 21.6‰ at 51.5-45.5 Ma, which represents a change of 3.6‰ in 5.0 Myr, or ~0.7‰ Myr^{-1}, and (2) from ~22.0‰ to 21.0‰ at 2-0 Ma, which represents a change of 1.0‰ in 2.0 Myr, or ~0.5 Myr^{-1}. We agree that the maximum observed rate of change in sulfate $\delta^{34}S$ is $\leq$0.7‰ Myr^{-1} and have amended it accordingly. Although this is more accurate, it does not change the basic point that we are making—that the maximum observed rate of change for the Cenozoic is less than the theoretical maximum.

8. p13197 l17. Consider adding the work of Rudnicki et al. (2001).

Response: OK. This paper is now cited.

9. p13197 l27, Canfield and Teske (1996), and their data indicates a spread up to 70 permil.

Response: We stated that MSR fractionation is "typically ~30 to 60‰ in modern marine systems" and we stand by this statement. We do not deny that more extreme values (both lower and higher) have been reported in some studies.

10. p13198 l25, the works of Rees (1973) and Brunner and Bernasconi (2005) are important here too.

Response: OK. These papers are now cited.

11. p13199 1 para. Since this is a fairly exhaustive list of processes affecting S fractionation, the author may want to consider to add Eckert et al. (2011) who show that cell external sulfide may affect S-fractionation (see also Brunner and Bernasconi, 2005).

Response: OK. This process and a citation to Eckert et al. (2011) have been added.

12. p13201 l 2, add citation for the Lowess model.

Response: The reader is already referred to Song et al. (2014), a study that provides both the algorithms and references to background material on LOWESS estimation. Additional documentation is not needed.

13. p13202 l5ff, p13204, The Song et al. (2014) data suggests that the Permo-Triassic concentrations must have been low?

Response: Yes, and this is discussed on p13206 l27-28 and p13207 l1-3, with data given in Table A4 and illustrated in Figure 8.

14. p13207 l9, Canfield and Teske 1996, and the values reported there seem to go up to 70 permil?

Response: We agree that the natural SRM populations documented by Canfield and Teske (1996) exhibit fractionations up to 70‰, although these populations display a distinct mode at 40-60‰. Our citation of a range of 30-60‰ was based on the average fractionations given in Table A1, so we have deleted the reference to Canfield and Teske (1996) and cited our Table A1. It should also be noted that the 30-60‰ range cited here represents typical marine MSR fractionation values, not the full range of reported values in nature (which would be larger).

15. p13207 l20ff If I understand this correctly, the rate based estimate really only works if the rate of change equals the residence time. If it is slower, or faster, this approach will fail. It might be useful to rephrase the discussion in the more general framework of residence time vs, rate of change.

Response: This question was fully addressed above.

16. p13209 l 5ff. I am not sure that I understand this argument. While I can see that the difference between CAS and Pyrite may be affected by the local hydrogeography, the sulfur data published by Paytan et al. (1998) are from coring locations in the Pacific, and as such not affected by local restriction. So the rate method should apply here.

Response: The discussion of South Atlantic paleohydrography on these lines does not refer to the Paytan et al. (1998) dataset but to that of Wortmann and Chernyavsky (2007), which is from a site in the South Atlantic. This paper is cited in the text, but the sources of data in Table A4

were inadvertently left out, which may have confused the reviewer. We have restored the sources of data to Table A4.

17. Last but not least, it would be useful if the authors provide their p-values for their regression model, as the r2-value only describes how good the fit is, but says nothing about how probable the model is.

Response: The r^2 values reported here are all high (0.74 to 0.80) and the number of samples large (n = 31 to 81)—consequently, the associated alpha errors ($p(\alpha)$) are all <0.01. We thought that this would be obvious to readers, but we have added $p(\alpha)$ values wherever r^2 is reported.

References cited

Algeo, T. J., Luo, G. M., Song, H. Y., Lyons, T. W. and Canfield, D. E.: Reconstruction of secular variation in seawater sulfate concentrations. Biogeosci. Disc., 11, 13187-13250, 2014.

Brunner, B. and Bernasconi, S. M.: A revised isotope fractionation model for dissimilatory sulfate reduction in sulfate reducing bacteria. Geochim. Cosmochim. Acta, 69(20), 4759-4771, 2005.

Canfield, D. E. and Teske, A.: Late Proterozoic rise in atmospheric oxygen concentration inferred from phylogenetic and sulfur isotope studies. Nature, 328, 127-132, 1996.

Demicco, R. V., Lowenstein, T. K., Hardie, L. A. and Spencer, R. J.: Model of seawater composition for the Phanerozoic. Geology, 33(11), 877-880, 2005.

Eckert, T., Brunner, B., Edwards, E. A. and Wortmann, U. G.: Microbially mediated re-oxidation of sulfide during dissimilatory sulfate reduction by *Desulfobacter latus*. Geochim. Cosmochim. Acta, 75(12), 3469-3485, 2011.

Lowenstein, T. K., Timofeef, M. N., Brennan, S. T., Hardie, L. A. and Demicco, R. V.: Oscillations in Phaneroizoic seawater chemistry: Evidence from fluid inclusions. Science, 294, 1086-1088, 2001.

Lowenstein, T. K., Hardie, L. A., Timofeef, M. N. and Demicco, R. V.: Secular variation in seawater chemistry and the origin of calcium chloride basinal brines. Geology, 31(10), 857-860, 2003.

Paytan, A., Kastner, M., Campbell, D. and Thiemens, M. H.: Sulfur isotopic composition of Cenozoic seawater sulfate. Science, 282, 1459-1462, 1998.

Paytan, A., Kastner, M., Campbell, D. and Thiemens, M. H.: Seawater sulfur isotope fluctuations in the Cretaceous. Science, 304, 1663-1665, 2004.

Rees, C. E.: A steady-state model for sulphur isotope fractionation in bacterial reduction processes. Geochim. Cosmochim. Acta, 37, 1141-1162, 1973.

Rudnicki, M. D., Elderfield, H. and Spiro, B.: Fractionation of sulfur isotopes during bacterial sulfate reduction in deep ocean sediments at elevated temperatures. Geochim. Cosmochim. Acta, 65(5), 777-789, 2001.

Song, H., Tong, J., Algeo, T. J., Song, H., Qiu, H., Zhu, Y., Tian, L., Bates, S., Lyons, T. W., Luo, G. and Kump, L. R.: Early Triassic seawater sulfate drawdown. Geochim. Cosmochim. Acta, 128, 95-113, 2014.

Wortmann, U. G. and Chernyavsky, B. M.: Effect of evaporite deposition on Early Cretaceous carbon and sulphur cycling. Nature, 446, 654-656, 2007.

Wortmann, U. G. and Paytan, A.: Rapid variability of seawater chemistry over the past 130 million years. Science, 337(6092), 334-336, 2012.

Wu, N., Farquhar, J., Strauss, H., Kim, S.-T. and Canfield, D. E.: Evaluating the S-isotope fractionation associated with Phanerozoic pyrite burial. Geochim. Cosmochim. Acta, 74, 2053-2071, 2010.

Comments by Anonymous Reviewer

Overview

Algeo et al. reconstruct ancient seawater sulfate concentrations using two simplistic yet elegant approaches applied to available data sets spanning back to the late Precambrian. These two approaches include 1) a "rate" method that takes advantage of the rate of sulfate sulfur isotope variability through time and 2) a microbial sulfate reduction (MSR) fractionation method that relates the degree of fractionation to absolute sulfate concentrations. Both stem from previously developed approaches, however here the authors take the next step and apply modified empirical/theoretical relationships to geochemical data preserved in the rock record. I commend the authors' efforts and broadly agree with the potential utility of their approaches, however important issues deserve detailed discussion.

Response: We thank the reviewer for these positive comments.

General Comments

Rate method. The application of modern S fluxes and associated δ34S values to ancient systems is likely an over-extension and probably produces some of the uncertainty (and some of the unrealistic values) in reconstructed sulfate concentrations. Whereas there are ways to get at output $\delta^{34}S$ (through $\delta^{34}Spyr$, for example), it is quite difficult to accurately predict the source $\delta^{34}S$. Indeed, previous authors infer that the sulfur isotope composition of the source flux has differed from modern values quite significantly (e.g., Fike and Grotzinger, 2008). To a first order, it is hard to envision the source $\delta^{34}S$ value as invariant over long timescales. Changes in the fractional burial of S as pyrite and sulfate minerals through time (thought to drive much of the marine sulfate $\delta^{34}S$ variability) almost requires a change in the source as rocks of differing ages are later weathered on land in different proportions. Ultimately, it would be useful if the authors included model sensitivity analyses to changing source $\delta^{34}S$.

Response: We agree that source flux $\delta^{34}S$ has probably varied through time, and that such variation may have influenced the $\delta^{34}S$ of seawater sulfate. We also agree that sensitivity analysis might be applied to test the potential influence of the source flux on seawater sulfate $\delta^{34}S$. However, this is beyond the scope of the present study. Our rate method (Equations 2-4) does not depend on source flux $\delta^{34}S$, so there is no need to engage in this exercise.

MSR method. The linear relationship between $\Delta^{34}S$sulfate-sulfide from modern aqueous systems is striking and suggests that there is hope in reconstructing ancient seawater sulfate concentrations with this approach. It would be useful if the authors distinguished which data points in Fig. 2 are derived from water column S phases, pore water S phases, solid S phase, etc. It seems somewhat coincidental that aqueous sulfate concentrations near the modern seawater sulfate concentration happen to yield the maximum $\delta^{34}S$, above which fractionations are essentially constant. Might the hypersaline environments explored be unrepresentative due to high ionic strength or some other dissolved constituent that limits isotopic discrimination? In

other words, can we be certain based on the current data set that seawater with higher sulfate contents (>29 mM) would not exhibit higher fractionations?

Response: In Figure 2, all sulfate $\delta^{34}S$ values used in calculation of $\Delta^{34}S_{sulfate\text{-}sulfide}$ are based on measurements of aqueous sulfate, as stated in the text. For sulfide $\delta^{34}S$, we used four different sulfur phases: pyrite, sediment acid-volatile sulfur (AVS), sediment total reduced sulfur (TRS), and aqueous H_2S (note: this information has been added to the sulfide $\delta^{34}S$ column of Table A1). At the reviewer's request, we have constructed a version of Figure 2 that shows the different sulfide phases, and we calculated separate regressions for each phase (Fig. B3). The following points should be noted about this figure. First, each of the four phases yields a statistically significant regression (r = 0.81-0.92; $p(\alpha)$ <0.05; see Table B1 below). Second, the four phases have similar regression slopes although slightly variable y-intercepts. For this reason, TRS and AVS yield $\Delta^{34}S_{CAS\text{-}PY}$ values that are, on average, slightly larger for a given $[SO_4^{2-}]_{SW}$ value than pyrite and aqueous H_2S. Third, the four regression lines generally converge at higher $[SO_4^{2-}]_{SW}$, and the largest differences occur at low $[SO_4^{2-}]_{SW}$, where data is sparser. Whether there are real differences in the regression relationships among these four sulfide phases is an issue that will require further inquiry—the regression lines in Figure B3 are not statistically different. One could argue in favor of using the pyrite $\delta^{34}S$ data alone, which would result in a small change in the regression relationship used to calculate paleoseawater $[SO_4^{2-}]_{SW}$ values. We opted to use a larger sulfide $\delta^{34}S$ dataset, especially one containing more data at low $[SO_4^{2-}]_{SW}$, in order to generate a stable relationship over a wider range of $[SO_4^{2-}]_{SW}$ values.

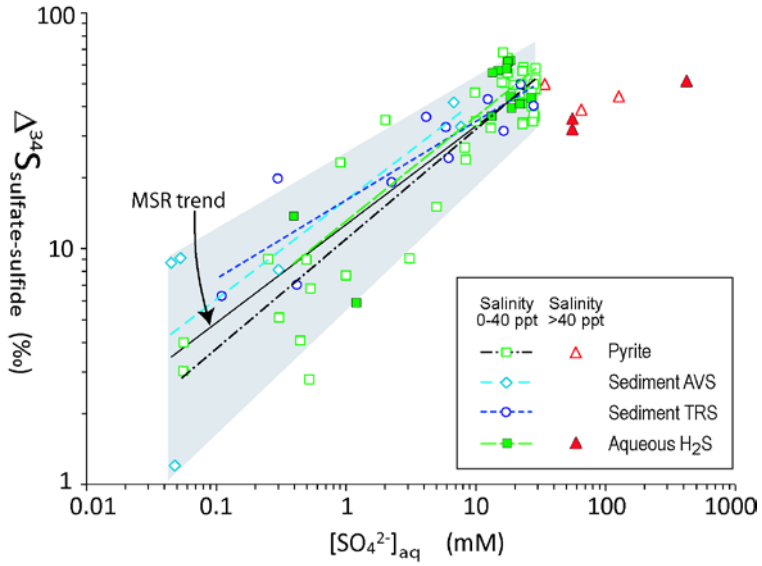

Figure B3

Figure B3. The MSR trend data of Algeo et al. (2014; their Figure 2 and Table A1) replotted as a function of sulfide $\delta^{34}S$ source (symbols as given in legend). Separate regressions for the four different sulfide phases (dashed lines) show small differences in slopes and y-intercepts (Table B1), although the lines are statistically indistinguishable.

Table B1. Regression statistics for reduced sulfur phases used in calculation of $\Delta^{34}S_{sulfate\text{-}sulfide}$

Sulfur phase	*n*	*r*	*m*	*b*	*p(α)*
Pyrite	48	0.92	0.46	-0.35	<0.01
Sediment AVS	6	0.81	0.42	-0.06	<0.05
Sediment TRS	11	0.89	0.33	0.20	<0.01
Aqueous H_2S	16	0.84	0.44	-0.20	<0.01

The second part of the reviewer's comment concerns the reasons why the hypersaline environments in our dataset (Table A1) do not conform to the 'MSR trend', i.e., the regression relationship for environments with salinities of <40 psu (= practical salinity units) (Fig. 2). Whether MSR fractionations reach a maximum at the salinity of modern seawater (35 psu) and then remain essentially unchanged at higher salinities is uncertain. Our dataset certainly suggests that this might be the case, but the number of examples of hypersaline environments (n = 6) is too small to reach firm conclusions. Because we are not even certain that the MSR fractionation trend changes above 35 psu, it would not be useful to speculate on what factors might make this small set of hypersaline environments "unrepresentative". We simply raise the possibility of a change in the MSR fractionation trend at salinities >40 psu with the intention of encouraging further research into this issue.

Action: We have added a brief mention of these issues to the text of the manuscript and an extended discussion as Appendix B of the revised manuscript. We did not insert this material into the text as it is of tangential importance to the development of the main theme of our paper.

Reliability of CAS and pyrite $\delta^{34}S$ as accurate, whole-ocean proxies. The modern global open ocean $\delta^{34}S$ value is derived from barite records (Paytan et al., 1998; 2004). However much of the ancient sulfate record, particularly the early Paleozoic and Neoproterozoic, is derived from carbonate platform CAS. It has yet to be demonstrated that these two records agree. Early work by Burdett et al. (1989) suggests that foraminifera CAS records agree with the Neogene barite record, but they analyzed pelagic planktonic foraminifera more closely associated with open ocean environments and not margin platforms. Lyons et al. (2004) show that very recent carbonate platform muds conform to the modern marine $\delta^{34}S$sulfate record, but these do not extend very far back in time. The authors do a good job critically choosing specific sulfur phases (e.g., shallow pyrite) to construct the MSR method equations. Whereas, modern environments provide the opportunity to be picky, ancient environments can only be probed through rock-bound proxies. Pyrite records are particularly sensitive in this regard, how can we be confident that the rock-bound pyrite is in fact shallow and therefore that $\Delta^{34}S$(CAS-pyr) accurately reflects cogenetic $\Delta^{34}S$sulfate-sulfide?

Response: First, fractionation of S isotopes during precipitation of sulfate evaporites and incorporation of CAS in carbonates has been shown to be small (<1‰) (Schidlowski et al., 1977;

Burdett et al., 1989; Kampschulte et al., 2001). The Phanerozoic records of CAS $\delta^{34}S$ and evaporite $\delta^{34}S$ were compared by Kampschulte and Strauss (2004), who found considerable overlap and no systematic bias toward higher values in one or the other dataset.

Second, we agree that the type of pyrite present in ancient sediments needs to be evaluated in order to assess whether it is syngenetic/early diagenetic and, thus, useful for calculating paleoseawater sulfate concentrations. There are well-established petrographic and geochemical techniques for this type of evaluation (e.g., Wilkin et al., 1996; Lyons and Severmann, 2006). This is an issue that each researcher making use of the methods developed in this study for estimation of paleoseawater sulfate concentrations will need to consider in regard to his/her specific study units.

Action: We have added a brief synthesis of these points to the manuscript.

Heterogenous marine $\delta^{34}S$ records. Unfortunately, $\delta^{34}S$ records of most time intervals have only been developed from one or two locations. The multiple records from the Neoproterozoic indicate both lateral (horizontal; Loyd et al., 2012; 2013) and stratified type (vertical; Li et al., 2010) variability probably stemming from overall low, but likewise variable, marine sulfate concentrations (as the authors mention, P13209-10; lns 34-30, 1-7). Similar heterogeneity may occur during other time intervals as well. In the face of potentially large heterogeneity, how reflective is a single succession of the global ocean? Furthermore, how can we be confident that intervals with data from only one or two successions can be used to accurately constrain a global signal?

Response: We agree that spatial heterogeneity in seawater sulfate concentrations may become pronounced at low average concentrations, as during the Neoproterozoic. This does not invalidate an estimate of seawater sulfate concentrations for a particular time and locale. It does mean that a single estimate will not suffice to characterize seawater globally, and that a number of estimates from widely separated locales would be desirable to characterize the range of variation in seawater sulfate concentrations at a given time. These considerations in no way invalidate our methodology for estimating seawater sulfate concentrations.

Action: We have added a brief synthesis of these points to the manuscript.

Specific Comments

P 13191, lns 5-7: It seems difficult to rationalize such a broad statement. Local source $\delta^{34}S$ values and fluxes will be particularly influential, especially if low oceanic [SO_4^{2-}] lends to short residence times.

Response: Whether such a statement is overly broad or not depends on one's outlook—there is no inherently correct view on such a matter. We agree with the reviewer that local variations in sulfate concentration and isotopic composition will become more pronounced at low average concentrations. The significance of this point was considered in the preceding response.

P 13191, lns 16-20: Perhaps, at least this is generally assumed but not adequately substantiated. Some authors interpret variable source $\delta^{34}S$ during specific time intervals (Fike and Grotzinger, 2008).

Response: We agree that this inference has not been fully substantiated. However, in terms of controls on seawater sulfate $\delta^{34}S$, there is a lot more evidence to support variable sulfur burial fluxes rather than variable source $\delta^{34}S$ as the dominant source (e.g., Kampschulte and Strauss, 2004; Bottrell and Newton, 2006; Halevy et al., 2012; Song et al., 2014).

P 13191, ln 22: "Cogenetic" formation is difficult to prove, however the authors do attempt to get as close to cogenetic as possible through targeted data mining.

Response: We agree on both points.

P 13192, lns 8-10: The direction of isotopic change indicates which term goes to zero. A negative change indicates pyrite burial going to zero, a positive change indicates the sulfate source going to zero. This deserves an explicit mention.

Response: We are discussing the source flux specifically. We have changed the wording to reflect that the source flux is specifically meant here.

General Note: What about stratified water columns? Since the proxy records are based on pyrite are they more strongly influenced by bottom water conditions?

Response: In marine systems, stratified water columns will have no effect on dissolved sulfate because its residence time is sufficiently long that sulfate will be uniformly distributed vertically. With regard to pyrite, syngenetic pyrite can form in the anoxic deepwaters of stratified watermasses. However, fractionation of syngenetic pyrite and that of early-formed diagenetic pyrite (when formed in an open system) should be similar—the effect of sediment on porewater chemistry is limited until permeability is reduced significantly.

P 13192, lns 24-25: Nor has the pyrite flux gone to zero.

Response: This comment is cryptic—we cannot comment.

P 13194, lns 19-21: But what's important is that shallow pyrite hasn't experienced overgrowth of more isotopically enriched pyrite formed in deeper, closed-system sediments. Also, it seems like shallow AVS would be the best target based on this argument. Ultimately, pyrite must be used because that's what is preserved in the geologic record.

Response: We agree with all of these comments. However, these issues are already adequately addressed in the manuscript.

P 13195, ln 7: This mathematical relationship is only valid if the original fluid is sourced from seawater. What about mixing with saline, non-seawater fluids?

Response: This relationship is valid for mixed fluids that contain a seawater component ≥5% (where the second fluid is low-sulfate freshwater). It would not be valid for a purely terrestrially sourced fluid. Sulfate concentrations for all freshwater systems in our dataset (Table A1, records 1-18) were measured, not calculated from salinity. Of the 36 brackish systems in our dataset (Table A1, records 19-54), we estimated sulfate concentrations for 9 of them from salinity data. By definition, our brackish systems had total salinities of 10 to 30 psu and thus consisted of 28-86% seawater. The calculated sulfate concentrations are therefore reliable—there are no problems with the sulfate concentrations in our dataset (Table A1).

P 13196, lns 3-5: The Habicht et al. (2002) data show a clear step function, not a linear relationship as seen in the natural samples.

Response: The statement in question is: "Our results are similar to, although more linear and more statistically robust than, those reported by Habicht et al. (2002) on the basis of culture experiments." Our results are similar to those of Habicht et al. in terms of the broad relationship between MSR fractionation and aqueous sulfate concentration, although more linear (as noted by the reviewer). We stand by our statement.

General Note: It would be nice to see how water column sulfide compares to shallow pyrite in modern systems where both are measureable or have been measured. This would provide confidence in the use of pyrite as a "cogenetic" proxy.

Response: This is related to the request by this reviewer for a figure showing the different sulfide phases used in calculating $\Delta^{34}S_{sulfate\text{-}sulfide}$ (see above). This figure (Figure B3) shows that the $\Delta^{34}S_{sulfate\text{-}sulfide}$-$[SO_4^{2-}]_{SW}$ relationships are similar for pyrite and aqueous H_2S. Although further detailed study might document a systematic offset between these sulfide phases, we cannot identify one in our dataset (Table B1).

P 13202, ln 21: The rate method-produced values may not be maxima, particularly if source $\delta^{34}S$ changes.

Response: The rate-method estimates are based on $\Delta^{34}S$(CAS-pyrite) and max($\partial SO_4^{2-}/\partial t$) (see Equations 2-4). They are not dependent on source $\delta^{34}S$. Variation in source $\delta^{34}S$ would matter only if average seawater sulfate concentrations were so low that seawater sulfate was no longer well-mixed globally.

P 13203, lns 1-4: I disagree. The further back in time, the less confidence we have in S flux magnitudes and isotopic compositions, accurate determination of which are required for a valid rate model.

Response: Sulfur isotopic fractionations ($\Delta^{34}S$(CAS-pyrite)) are quite well-determined for >2.3-Ga samples, being uniformly small (<4‰). The difficulty with rate estimates for samples this old is not the sulfur isotopic compositions but limited age control. With adequate age control, the rate method may be quite useful for very old samples. This is largely a matter of opinion—we respect the reviewer's but stand by our own.

P 13203, ln 7: Diagenesis may also homogenize $\delta^{34}S_{CAS}$ (and therefore reduce δ / $\delta t(max)$) depending on the nature of diagenetic fluids and the degree of recrystallization/alteration.

Response: We agree. Diagenesis was mentioned as an example of a process that might increase variance in $\delta^{34}S_{CAS}$, but it might also reduce variance. We have inserted a brief mention of this possibility.

P 13207 and throughout: Although it is difficult to reconstruct ancient [Ca^{2+}], very high values of [SO_4^{2-}] are unlikely because of the tendency to saturate the oceans with respect to anhydrite and gypsum. With a modern [Ca^{2+}] of ~10 mM and [SO_4^{2-}] of ~100 mM fluids will be supersaturated (by 30X levels pertaining to saturation). Is there an upper limit to sulfate concentrations that can be calculated?

Response: This is an interesting idea, and one that has been considered previously. Variation in seawater [Ca^{2+}] and [SO_4^{2-}] has been estimated for the Phanerozoic in at least three studies (Hardie, 1996; Horita et al., 2002; Lowenstein et al., 2003). We included some of the results of these studies in Figure 5 of our paper (Algeo et al., 2014).

P 13208, lns 22-24. A restricted basin may exhibit elevated or reduced sulfate concentrations. Restricted evaporative basins or those with limited reactive organic carbon may exhibit [SO_4^{2-}] above seawater due to evaporation and restriction of MSR, respectively.

Response: We agree. Such basinal watermass effects may underlie the unusual behavior exhibited by some of the Mesozoic units in our paper (Fig. 8; see discussion in Section 4.3).

References cited

Algeo, T. J., Luo, G. M., Song, H. Y., Lyons, T. W. and Canfield, D. E.: Reconstruction of secular variation in seawater sulfate concentrations. Biogeosci. Disc., 11, 13187-13250, 2014.

Bottrell, S. H. and Newton, R. J.: Reconstruction of changes in global sulfur cycling from marine sulfate isotopes. Earth-Sci. Rev., 75(1), 59-83, 2006.

Burdett, J. W., Arthur, M. A. and Richardson, A. A.: Neogene seawater sulfur isotope age curve from calcareous pelagic microfossils. Earth Planet. Sci. Lett., 94, 189-198, 1989.

Fike, D. A. and Grotzinger, J. P.: A paired sulfate-pyrite $\delta^{34}S$ approach to understanding the evolution of the Ediacaran–Cambrian sulfur cycle. Geochim. Cosmochim. Acta, 72, 2636-2648, 2008.

Habicht, K. S., Gade, M., Thamdrup, B., Berg, P. and Canfield, D. E.: Calibration of sulfate levels in the Archean ocean. Science, 298, 2372-2374, 2002.

Halevy, I., Peters, S. E. and Fischer, W. W.: Sulfate burial constraints on the Phanerozoic sulfur cycle. Science, 337(6092), 331-334, 2012.

Hardie, L. A.: Secular variation in seawater chemistry: An explanation for the coupled secular variation in the mineralogies of marine limestones and potash evaporites over the past 600 m.y. Geology, 24, 279-283, 1996.

Horita, J., Zimmermann, H. and Holland, H. D.: Chemical evolution of seawater during the Phanerozoic: Implications from the record of marine evaporites. Geochim. Cosmochim. Acta, 66(21):3733-3756, 2002.

Kampschulte, A., Bruckschen, P. and Strauss, H.: The sulphur isotopic composition of trace sulphates in Carboniferous brachiopods: implications for coeval seawater, correlation with other geochemical cycles and isotope stratigraphy. Chem. Geol., 175, 149-173, 2001.

Kampschulte, A. and Strauss, H.: The sulfur isotopic evolution of Phanerozoic seawater based on the analysis of structurally substituted sulfate in carbonates. Chem. Geol., 204, 255-286, 2004.

Li, C., Love, G. D., Lyons, T. W., Fike, D. A., Sessions, A. L. and Chu, X.: A stratified redox model for the Ediacaran ocean. Science, 328, 80-83, 2010.

Lowenstein, T. K., Hardie, L. A., Timofeef, M. N. and Demicco, R. V.: Secular variation in seawater chemistry and the origin of calcium chloride basinal brines. Geology, 31(10), 857-860, 2003.

Loyd, S. J., Marenco, P. J., Hagadorn, J. W., Lyons, T. W., Kaufman, A. J., Sour-Tovar, F. and Corsetti, F. A.: Sustained low marine sulfate concentrations from the Neoproterozoic to the Cambrian: insights from carbonates of northwestern Mexico and eastern California. Earth Planet. Sci. Lett., 339-340, 79-94, 2012.

Loyd, S. J., Marenco, P. J., Hagadorn, J. W., Lyons, T. W., Kaufman, A. J., Sour-Tovar, F. and Corsetti, F. A.: Local $\delta^{34}S$ variability in 580 Ma carbonates of northwestern Mexico and the Neoproterozoic marine sulfate reservoir. Precambr. Res., 224, 551-569, 2013.

Lyons, T. W. and Severmann, S.: A critical look at iron paleoredox proxies: New insights from modern euxinic marine basins. Geochim. Cosmochim. Acta, 70, 5698-5722, 2006.

Lyons, T. W., Walter, L. M., Gellatly, A. M., Martini, A. M. and Blake, R. E.: Sites of anomalous organic remineralization in the carbonate sediments of South Florida, USA: The sulfur cycle and carbonate-associated sulfate. In: Amend, J. P., Edwards, K. J. and Lyons, T. W. (eds.), Sulfur Biogeochemistry—Past and Present, Geol. Soc Am. Spec. Paper 379, 161-176, 2004.

Paytan, A., Kastner, M., Campbell, D. and Thiemens, M. H.: Sulfur isotopic composition of Cenozoic seawater sulfate. Science, 282, 1459-1462, 1998.

Paytan, A., Kastner, M., Campbell, D., and Thiemens, M. H.: Seawater sulfur isotope fluctuations in the Cretaceous. Science, 304, 1663-1665, 2004.

Schidlowski, M., Junge, C. E. and Pietrek, H.: Sulfur isotope variations in marine sulfate evaporites and the Phanerozoic oxygen budget. J. Geophys. Res., 82(18), 2557-2565, 1977.

Song, H., Tong, J., Algeo, T. J., Song, H., Qiu, H., Zhu, Y., Tian, L., Bates, S., Lyons, T. W., Luo, G. and Kump, L. R.: Early Triassic seawater sulfate drawdown. Geochim. Cosmochim. Acta, 128, 95-113, 2014.

Wilkin, R. T., Barnes, H. L. and Brantley, S. L.: The size distribution of framboidal pyrite in marine sediments: an indicator of redox conditions. Geochim. Cosmochim. Acta, 60, 3897-3912, 1996.

Reconstruction of secular variation in seawater sulfate concentrations

T.J. Algeo[1,2,3*], G.M. Luo[2], H.Y. Song[3], T.W. Lyons[4], and D.E. Canfield[5]

[1]Department of Geology, University of Cincinnati, Cincinnati, Ohio 45221-0013, U.S.A.
[2] State Key Laboratory of Geological Processes and Mineral Resources, China University of Geosciences, Wuhan, 430074, China
[3]State Key Laboratory of Biogeology and Environmental Geology, China University of Geosciences, Wuhan, 430074, China
[4]Department of Earth Sciences, University of California, Riverside, California 92521-0423, U.S.A.
[5]Nordic Center for Earth Evolution (NordCEE) and Institute of Biology, University of Southern Denmark, Campusvej 55, 5230 Odense M, Denmark

*Correspondence to: T. J. Algeo (Email: Thomas.Algeo@uc.edu)

Abstract

Long-term secular variation in seawater sulfate concentrations ($[SO_4^{2-}]_{SW}$) is of interest owing to its relationship to the oxygenation history of Earth's surface environment~~, but quantitative approaches to analysis of this variation remain underdeveloped~~. In this study, we develop two complementary approaches for ~~assessment of~~quantification of ~~the $[SO_4^{2-}]$ of~~sulfate concentrations in ancient seawater and test their application to ~~to reconstructions of $[SO_4^{2-}]_{SW}$ variation since the~~ late Neoproterozoic ~~Eon (<650~~635 Ma) to Recent marine units. The ~~first approach~~"rate method" is based on two measurable parameters of paleomarine systems: (1) the S-isotope fractionation associated with microbial sulfate reduction (MSR), as proxied by $\Delta^{34}S_{CAS\text{-}PY}$, and (2) the maximum rate of change in seawater sulfate, as proxied by $\partial\delta^{34}S_{CAS}/\partial t(max)$. ~~This "rate method" yields an estimate of the maximum possible $[SO_4^{2-}]_{SW}$ for the time interval of interest, although the calculated value differs depending on whether an oxic or an anoxic ocean model is inferred.~~ The "MSR-trend method" ~~second approach is also based on $\Delta^{34}S_{CAS\text{-}PY}$ but evaluates this parameter against an empirical MSR trend rather than a formation-specific $\partial\delta^{34}S_{CAS}/\partial t(max)$ value. The MSR trend~~ is based on the empirical relationship of $\Delta^{34}S_{CAS\text{-}PY}$ to ~~represents the relationship between fractionation of cogenetic sulfate and sulfide (i.e., $\Delta^{34}S_{sulfate\text{-}sulfide}$)~~ aqueous sulfate concentrations ~~and ambient dissolved sulfate concentrations~~ in 81 modern ~~aqueous~~ depositional systems. For a given paleomarine system, the rate method yields an estimate of maximum possible $[SO_4^{2-}]_{SW}$ (although results are dependent on assumptions regarding the pyrite burial flux, F_{PY}), and the MSR-trend method ~~. This "MSR-trend method" is thought to yield a robust~~yields an estimate of mean ~~seawater~~ $[SO_4^{2-}]_{SW}$ ~~for the time interval of interest~~. An analysis of seawater sulfate concentrations since 63550 Ma suggests that $[SO_4^{2-}]_{SW}$ was low during the late Neoproterozoic (<5 mM), rose sharply across the Ediacaran/Cambrian boundary (~~to~~ ~5-10 mM), and rose again during the Permian (~10-30 mM) to levels ~~(~10-30 mM)~~ that have varied only slightly since 250 Ma.

Formatted: Subscript

However, Phanerozoic seawater sulfate concentrations may have been drawn down to much lower levels (~1-4 mM) during short (<~2-Myr) intervals of the Cambrian, Early Triassic, Early Jurassic, ~~and possibly other intervals~~and Cretaceous as a consequence of widespread ocean anoxia, intense MSR, and pyrite burial. The procedures developed in this study offer potential for future high-resolution quantitative analyses of paleoseawater sulfate concentrations.

Keywords: Phanerozoic; Neoproterozoic; microbial sulfate reduction; pyrite; carbonate-associated sulfate; sulfur cycle

1 Introduction

Oceanic sulfate plays a key role in the biogeochemical cycles of S, C, O and Fe (Canfield, 1998; Lyons and Gill, 2010; Halevy et al., 2012; Planavsky et al., 2012). For example, >50% of organic matter and methane in marine sediments is oxidized via processes linked to microbial sulfate reduction (MSR) (Jørgensen, 1982; Valentine, 2002). At a concentration of ~29 mM in the modern ocean, sulfate is the second most abundant anion in seawater (Millero, 2005). Its concentration is an important proxy for seawater chemistry and the oxidation state of the Earth's atmosphere and oceans (Kah et al., 2004; Johnston, 2011).

Formatted: Space Before: 6 pt, After: 6 pt

Although there is broad agreement that seawater sulfate concentrations have increased through time, the history of its accumulation remains poorly known in detail. Archean and Early Proterozoic oceans are thought to have had very limited sulfate inventories (<200 μM), as implied by small degrees of sulfate-sulfide and mass-independent S-isotope fractionation (Shen et al., 2001; Strauss, 2003; Farquhar et al., 2007; Adams et al., 2010; Johnston, 2011; Owens et al., 2013; Luo et al., 2015~~in review~~). The accumulation of atmospheric O_2 during the 'Great Oxidation Event' (~2.3-2.0 Ga; Holland, 2002; Bekker et al., 2004) is thought to have resulted in a long-term increase in seawater sulfate concentrations (Canfield and Raiswell, 1999; Canfield et al., 2007; Kah et al., 2004; Fike et al., 2006). However, this increase was probably not monotonic and declines in pO_2 may have resulted in one or more seawater sulfate minima between ~1.9 and 0.6 Ga (Planavsky et al., 2012; Luo et al., 2015~~in review~~). Estimates of Phanerozoic seawater sulfate concentrations are uniformly higher, although there is no consensus regarding exact values. Fluid inclusion data yielded estimates of ~10 to 30 mM for most of the Phanerozoic (Horita et al., 2002; Lowenstein et al., 2003, 200~~3~~5). However, recent S-isotope studies have modeled concentrations as low as ~1-5 mM during portions of the Cambrian, Triassic, Jurassic, and Cretaceous (Wortmann and Chernyavsky, 2007; Adams et al., 2010; Luo et al., 2010; Gill et al., 2011a,b; Newton et al., 2011; Owens et al., 2013; Song et al., 2014), and a recent marine S-cycle model yielded low concentrations (<10 mM) for ~~the entire~~much of the Cretaceous and Early Cenozoic before a rise to near-modern levels at ~40 Ma (Wortmann and Paytan, 2012).

Formatted: Indent: First line: 0", Space After: 6 pt

Here, we develop two approaches for quantitative analysis of seawater sulfate concentrations ($[SO_4^{2-}]_{SW}$) in paleomarine systems. The first method calculates a maximum

Formatted: Space Before: 6 pt, After: 6 pt

possible $[SO_4^{2-}]_{SW}$ based on a combination of two parameters that are readily measurable in most paleomarine systems: (1) the S-isotope fractionation between cogenetic sedimentary sulfate and sulfide ($\Delta^{34}S_{CAS\text{-}PY}$), and (2) the maximum observed rate of variation in seawater sulfate $\delta^{34}S$ ($\partial\delta^{34}S_{CAS}/\partial t$). This "rate-based method" is an extension of earlier modeling work by Kump and Arthur (1999), Kurtz et al. (2003), Kah et al. (2004), Bottrell and Newton (2006), and Gill et al. (2011a,b). The second approach yields an estimate of mean seawater $[SO_4^{2-}]$ based on an empirical relationship between $\Delta^{34}S_{CAS\text{-}PY}$ and ambient dissolved aqueous sulfate concentrations (the "MSR trend") in 81 modern aqueous depositional systems (the MSR trend). Conceptually, the is "MSR-trend method" is thus based on an updated version of related to the the fractionation relationship that was quantified bygiven in Habicht et al. (2002; their figure 1). Although some earlier studies have Whereas earlier analyses commonly made qualitative assessments of paleo-seawater $[SO_4^{2-}]$ (e.g., Luo et al., 2010), the significance of our methodology is that the $[SO_4^{-2}]$ of ancient seawater can be quantitatively constrained as a function of measurable sediment parameters and empirical fractionation relationships.

We fully recognize that the marine sulfur cycle is controlled by myriad factors, many of which are only now coming to light thanks to detailed field and laboratory studies, and that not all such influences can be thoroughly considered and accommodated in the present study. While acknowledging the complexity of the sulfur cycle, this paper study attempts to identify broad first-order trends that potentially transcend these diverse influences and that are robust over significant intervals of geologic time. Our ultimate goal is to generate useful approximations of the long-term history of sulfate in the ocean. Our results suggest that large-scale empirical relationships may exist that are not highly sensitive to local controls such as ratesinfluences such as organic substrate type, of MSR,sulfate reduction rates syngenetic versus diagenetic pyrite formation, strain-specific isotopic behaviorfractionation, among othersand other factors. We envision such local influences, as they become more completely understood, being mapped onto, and thus integrated with, the broad first-order relationships documented hereinin this study.

2 Methods of modeling paleo-seawater sulfate concentrations

2.1 The rate method

The marine S cycle has a limited number of fluxes with fairly well-defined S-isotope ranges (Holser et al., 1989; Canfield, 2004; Bottrell and Newton, 2006), making it and, thus, is amenable to analysis through modeling (e.g., Halevy et al., 2012). Subaerial weathering yields a riverine sulfate source flux (F_Q) of ~10 x 10^{13} g yr^{-1} with an average $\delta^{34}S$ of ~+6‰, which is significantly lighter than the modern seawater sulfate $\delta^{34}S$ of +20‰. Sulfate is removed to the sediment either in an oxidized state, as carbonate-associated sulfate (CAS) or evaporite deposits, or in a reduced state, mainly as FeS or FeS_2. The oxidized sink has a flux (F_{EVAP}) of ~6 x 10^{13} g yr^{-1} with a S-isotopic composition that closely mimics that of coeval seawater ($\Delta^{34}S_{SW\text{-}EVAP}$ of -4 to 0‰). The reduced sink has a flux (F_{PY}) of ~4 x 10^{13} g yr^{-1} with a composition that characteristically shows a large negative fractionation relative to coeval seawater ($\Delta^{34}S_{sulfate}$SW-

Formatted: Indent: First line: 0", Space After: 6 pt

Formatted: Space After: 6 pt

Formatted: Space After: 6 pt

sulfide~~PY~~ of ~30 to 60‰; Habicht and Canfield, 1997; Canfield, 2001; Brüchert, 2004; Brunner and Bernasconi, 2005). Secular variation in seawater sulfate $\delta^{34}S$ is mainly due to changes in the relative size of the sink fluxes, with increasing (decreasing) burial of pyrite relative to sulfate leading to more (less) ^{34}S-enriched seawater sulfate (Holser et al., 1989; Bottrell and Newton, 2006; Halevy et al., 2012).

The rate method calculates a~~We adapted the models of Kurtz et al. (2003) and Kah et al. (2004) in order to calculate~~ maximum ~~ancient~~ seawater sulfate concentration~~s~~ ($[SO_4^{2-}]_{SW}$(max))~~)~~ based on two parameters: (1) S-isotope fractionation between cogenetic sedimentary sulfate and sulfide ($\Delta^{34}S_{sulfate\text{-}sulfide}$, as proxied by $\Delta^{34}S_{CAS\text{-}PY}$), and (2) the maximum observed rate of variation in seawater sulfate S isotopes ($\partial\delta^{34}S_{SO4}/\partial t$(max), as proxied by $\partial\delta^{34}S_{CAS}/\partial t$(max)) (Fig. 1). Rates of isotopic change for seawater sulfate are given by:

$$\partial\delta^{34}S_{CAS}/\partial t = ((F_Q \times \Delta^{34}S_{Q\text{-}SW}) - (F_{PY} \times \Delta^{34}S_{CAS\text{-}PY})) / M_{SW} \quad (1)$$

where $F_Q \times \Delta^{34}S_{Q\text{-}SW}$ is the flux-weighted difference in the isotopic compositions of the source flux and seawater (SW), $F_{PY} \times \Delta^{34}S_{CAS\text{-}PY}$ is the flux-weighted difference in the isotopic compositions of the reduced-S sink flux and seawater, and M_{SW} is the mass of seawater sulfate. The full expression represents the time-integrated influence of the source and sink fluxes on seawater sulfate $\delta^{34}S$. The maximum possible rate of change in the sulfur isotopic composition of seawater sulfate is attained when ~~one of the fluxes (e.g., the~~ source flux~~, as in Eq. 2)~~ goes to zero:

$$\partial\delta^{34}S_{CAS}/\partial t(max) = F_{PY} \times \Delta^{34}S_{CAS\text{-}PY} / M_{SW} \quad (2)$$

Reorganization of this equation allows calculation of a maximum seawater sulfate concentration from measured values of $\Delta^{34}S_{CAS\text{-}PY}$ and $\partial\delta^{34}S_{CAS}/\partial t$(max):

$$M_{SW} = k_1 \times F_{PY} \times \Delta^{34}S_{CAS\text{-}PY} / \partial\delta^{34}S_{CAS}/\partial t(max) \quad (3)$$

$$[SO_4^{2-}]_{SW}(max) = k_2 \times M_{SW} \quad (4)$$

where k_1 is a unit-conversion constant equal to 10^6, and k_2 is a constant relating the mass of seawater sulfate to its molar concentration that is equal to 2.~~15~~22 x 10^{-20} mM g^{-1}. Kah et al. (2004) ~~used~~ assumed F_{PY} = 10 x 10^{13} g yr^{-1}, which is the total sink flux for modern seawater sulfate, in order to model $\partial\delta^{34}S_{CAS}/\partial t$(max). While this may be appropriate for intervals of widespread euxinia in the global ocean, F_{PY} = 4 x 10^{13} g yr^{-1} (i.e., the modern ~~value~~sink flux) may better represent intervals with well-oxygenated oceans in which the sink fluxes of sulfate S and pyrite S are ~~subequal~~ both substantial (Fig. 1). Assuming F_{PY} = 4 x 10^{13} g yr^{-1}~~For~~ and values of $\Delta^{34}S_{CAS\text{-}PY}$ and $\partial\delta^{34}S_{CAS}/\partial t$(max) potentially ~~that are potentially~~ representative of ~~the~~ modern ~~ocean~~ marine systems (e.g., 35‰ and 1.1‰ Myr^{-1}~~; see discussion below~~, respectively)~~)~~, Equation~~.~~ 3 yields the modern seawater sulfate mass of M_{SW} = 1.3 x 10^{21} g ~~(assuming F_{PY} = 4 x 10^{13} g yr^{-1}),~~ and Equation~~.~~ 4 yields the modern seawater sulfate concentration of ~29 mM ~~(Millero, 2005)~~.

Relationships among the rate-method ~~model~~ parameters are illustrated in Figure 1 for $\Delta^{34}S_{CAS\text{-}PY}$ from 1 to 100‰ (ordinal scale) and for discrete values of $\partial\delta^{34}S_{CAS}/\partial t$(max) ranging from 1 to 100‰ Myr^{-1} (diagonal lines). $[SO_4^{-2}]_{SW}$ increases linearly with increasing $\Delta^{34}S_{CAS\text{-}PY}$ (at constant $\partial\delta^{34}S_{CAS}/\partial t$(max)) and decreases linearly with increasing $\partial\delta^{34}S_{CAS}/\partial t$(max) (at constant

Formatted: Space After: 6 pt

$\Delta^{34}S_{CAS\text{-}PY}$). The ~~observed~~ *measured* maximum $\partial\delta^{34}S_{CAS}/\partial t$ for a paleomarine unit is generally smaller than the *theoretical* maximum $\partial\delta^{34}S_{SO4}/\partial t$ because the latter can be achieved only when the source flux of seawater ~~sulfate~~ sulfur is reduced (at least transiently) to zero (Kah et al., 2004), which does not routinely occur in nature. As a consequence, rate-method estimates of $[SO_4^{2-}]_{SW}$ ~~for a given paleomarine system~~ are generally ~~are~~ larger than actual seawater sulfate concentrations, so Eq~~.~~uation 4 yields the *maximum* likely $[SO_4^{2-}]_{SW}$ for a paleomarine unit ~~n interval~~ of interest. This outcome can be~~is~~ illustrated by a calculation for the modern ocean, using $\Delta^{34}S_{CAS\text{-}PY}$ of ~30-60‰ ~~(e.g., Canfield and Thamdrup, 1994)~~ and $\partial\delta^{34}S_{CAS}/\partial t$(max) of ~0.~~5~~7‰ Myr^{-1} (based on the Cenozoic seawater sulfate $\delta^{34}S$ record; Paytan et al., 1998). These inputs yield $[SO_4^{2-}]_{SW}$(max) values between ~40 and ~~120~~ 80 mM, which is modestly larger than the actual modern $[SO_4^{2-}]_{SW}$ of ~29 mM (Fig. 1). Overestimation of modern $[SO_4^{2-}]_{SW}$ is due to ~~the fact that observed~~ measured $\partial\delta^{34}S_{CAS}/\partial t$ values for the Cenozoic ~~are just~~(~~<~~0.7‰ Myr^{-1}~~<0.5‰ Myr^{-1}~~) ~~and, thus, have not approached~~being lower than the theoretical maximum for modern seawater (~1-2‰ Myr^{-1}; Fig. 1). This situation is probably typical ~~of the marine sulfur cycle through time~~of marine units of all ages—~~maximum observed~~ measured ~~rates of ∂~~rates of $\delta^{34}S_{CAS}$ variation~~/∂t~~ ~~are~~ will ~~generally going to~~ be lower than the theoretical maximum ~~*theoretical* rates~~ because the source flux of sulfur to the oceans ~~has probably never gone~~rarely if ever goes to zero ~~(as modeled in Eq. 2)~~.

The results of the rate method depend on the parameterization of the pyrite burial flux (F_{PY}). This method is likely to yield an accurate estimate of seawater sulfate concentrations only if F_{PY} is inversely proportional to the residence time of sulfate in seawater (τ_{SO4}), which basically requires the marine sulfate system to be in equilibrium. If a value for F_{PY} is chosen that is much larger or smaller than the equilibrium flux, then seawater sulfate concentrations will be overestimated or underestimated, respectively (see Appendix B1 for extended discussion). Second, the pyrite burial flux has almost certainly varied through time. Since pyrite burial flux is a component of Equations 2 and 3, variations in this parameter will influence calculated seawater sulfate concentrations. Phanerozoic variation in pyrite burial fluxes has been calculated in several global carbon-sulfur cycle models (e.g., Berner, 2004; Bergmann et al., 2004), although the details remain unpublished. We therefore explored the effects of variable pyrite burial fluxes on seawater sulfate estimates by using the $[SO_4^{2-}]_{SW}$-dependent pyrite burial flux relationship of Wortmann and Chernyavsky (2007). This procedure yielded Phanerozoic $[SO_4^{2-}]_{SW}$ estimates that are close (±10%) to our original values (see Appendix B2 for extended discussion).

2.2 The MSR-trend method

An alternative approach to constraining ancient seawater sulfate concentrations is based on an empirical relationship~~s with~~ to ~~the~~ S-isotope fractionation associated with microbial sulfate reduction (F_{MSR}). We evaluated this relationship by compiling $\Delta^{34}S_{sulfate\text{-}sulfide}$ and $[SO_4^{2-}]_{aq}$ data for 81 ~~examples from~~ modern ~~aqueous~~ depositional systems~~, including freshwater, brackish, marine, and hypersaline environments~~ (Table A1; cf. Habicht et al., 2002). Each system was classified (1) by salinity, as freshwater (<10 psu), brackish (10-30 psu), marine (30-40 psu), or

Formatted: Font color: Auto
Formatted: Font color: Auto
Formatted: Font: Not Italic
Formatted: Font: Not Italic
Formatted: Space Before: 0 pt
Formatted: Subscript
Formatted: Font color: Auto
Formatted: Font color: Auto
Formatted: Font color: Auto
Formatted: Font color: Auto
Formatted: Font color: Auto
Formatted: Subscript
Formatted: Font color: Auto
Formatted: Font color: Auto
Formatted: Font color: Auto
Formatted: Font color: Auto
Formatted: Font color: Auto
Formatted: Font color: Auto
Formatted: Font color: Auto
Formatted: Font color: Auto
Formatted: Font color: Auto
Formatted: Font color: Auto
Formatted: Font color: Auto
Formatted: Font color: Auto
Formatted: Font color: Auto
Formatted: Font color: Auto
Formatted: Font color: Auto
Formatted: Font color: Auto
Formatted: Font color: Auto
Formatted: Font color: Auto
Formatted: Font color: Auto
Formatted: Space After: 6 pt

hypersaline (>40 psu; n.b., psu = practical salinity units), and (2) by redox conditions, as oxic or euxinic depending on whether the chemocline was within the sediment or the watermass, respectively.

In the interests of applying uniform criteria to the generation of this dataset, we followed a specific protocol. ~~Third~~First, we adopted a modern seawater sulfate concentration of 2775 mg L^{-1}, ~~-~~or 28.9 mM at~~(given~~ an average seawater density of 1025 kg m^{-3}~~)~~ (Millero, 2005). For brackish marine watermasses~~non-marine settings~~, we used measured aqueous sulfate concentrations or, ~~wherever~~ if unavailable, estimated ~~. Where unavailable for brackish or hypersaline marine systems, we calculated~~ dissolved sulfate concentrations from salinity data:

$$[SO_4^{2-}] = [SO_4^{2-}]_{SW} \times S / S_{SW} \quad (5)$$

where $[SO_4^{2-}]$ and S are the sulfate concentration and salinity of the watermass of interest, respectively, and S_{SW} is the salinity of average seawater (35 psu). ~~Some secular variation in the salinity and, hence, aqueous sulfate concentration of non-marine and restricted-marine watermasses is likely, but its potential effect on the F_{MSR}-$[SO_4^{2-}]_{aq}$ relationship may be limited.~~~~First~~Second, we used only in-situ water-column measurements of aqueous sulfate $\delta^{34}S$ ~~for aqueous sulfate~~. ~~Second~~Third, we used sulfide $\delta^{34}S$ values either from aqueous H_2S or from sedimentary sulfide proxies located ~~used in-situ water-column or~~within a few centimeters of the sediment-water interface, thus avoiding ~~uppermost sediment-porewater measurements of $\delta^{34}S$ for aqueous sulfide or, if lacking, measurements of $\delta^{34}S$ of sedimentary sulfide as a proxy for aqueous sulfide. Because solid-phase~~ sedimentary sulfides ~~generally exhibit a pronounced shift toward more~~that might be significantly ^{34}S-enriched ~~compositions under~~owing to sulfate-limited ~~(e.g., burial)~~ conditions (Kaplan et al., 1963; Canfield et al., 1992)~~, we used $\delta^{34}S$ values only from samples taken at or within a few centimeters of the sediment-water interface~~. However, some variation in $\delta^{34}S$ among cogenetic early-formed sedimentary sulfides is common. Acid-volatile sulfur (AVS, consisting mainly of monosulfides; Rickard, 1975) tends to have a ~~heavier~~lighter sulfur isotopic composition, closer to that of the instantaneously generated H_2S at a given sediment depth, because it converts quickly to pyrite ~~with burial~~ (Zaback and Pratt, 1992; Lyons, 1997). On the other hand, or~~, and or~~ganic ~~S~~sulfur tends to be isotopically heavier ~~possibly~~ owing to late-stage sulfurization of organic matter or, possibly,~~owing~~ to fractionations associated ~~with the sulfurization of organic matter~~with sulfur uptake (Zaback and Pratt, 1992; Werne et al., 2000, 2003, 2008). ~~Some variation in $\delta^{34}S$ among cogenetic sedimentary sulfides is common. Pyrite S is generally more ^{34}S-depleted than acid-volatile S (AVS) and organic S because it represents a time-integrated signal that incorporates early-generated, strongly ^{34}S-depleted H_2S (Kaplan et al., 1963; Canfield et al., 1992). On the other hand, AVS tends to have a heavier sulfur isotopic composition, closer to that of the instantaneously generated H_2S at a given sediment depth, because it converts quickly to pyrite with burial (Lyons, 1997), and organic S tends to be isotopically heavier possibly owing to fractionations associated with the sulfurization of organic matter (Werne et al., 2000, 2003, 2008). For these reasons, w~~Although our dataset includes~~ utilized~~ a combination of pyrite, AVS, total reduced sulfur (TRS), and ~~rather than AVS or other solid-phase sulfides as a proxy in~~

Formatted: Space After: 6 pt, Don't adjust space between Latin and Asian text, Don't adjust space between Asian text and numbers

Formatted: Subscript

estima aqueous H_2S ting aqueous sulfide $\delta^{34}S$sulfur isotopic data owing to variations in sample analysis among published studies, it is weighted toward pyrite data (n = 48 out of a total of 81; Table A1). An analysis of $\Delta^{34}S_{sulfate\text{-}sulfide}$ variation among the multiple sulfide sources used in our study revealed no statistically significant differences (see Appendix B3). Because pyrite $\delta^{34}S$ is frequently analyzed in paleomarine studies, our MSR trend (Fig. 2) should be widely applicable to an analysis of paleoseawater sulfate concentrations. --One caveat in this regard is that $\Delta^{34}S_{CAS\text{-}PY}$ estimates for paleomarine units should be based on syngenetic or early diagenetic pyrite, as determined by well-established petrographic and geochemical criteria (e.g., Wilkin et al., 1996; Lyons and Severmann, 2006).Third, we adopted a modern seawater sulfate concentration of 2775 mg L^{-1} or 28.9 mM (given a seawater density of 1025 kg m^{-3}) (Millero, 2005). For non-marine settings, we used measured aqueous sulfate concentrations wherever available. Where unavailable for brackish or hypersaline marine systems, we calculated dissolved sulfate concentration from salinity data:

$$[SO_4^{2-}] = [SO_4^{2-}]_{SW} \times S / S_{SW} \quad (5)$$

where $[SO_4^{2-}]$ and S are the sulfate concentration and salinity of the watermass of interest, respectively, and S_{SW} is the salinity of average seawater (35 psu). Some secular variation in the salinity and, hence, aqueous sulfate concentration of non-marine and restricted-marine watermasses is likely, but its potential effect on the F_{MSR}-$[SO_4^{2-}]_{aq}$ relationship may be limited.

The protocol described above produced an internally consistent dataset (Table A1) that exhibits a pronounced relationship between $\Delta^{34}S_{sulfate\text{-}sulfide}$ and $[SO_4^{2-}]_{aq}$ (Fig. 2a). Regression of $\Delta^{34}S_{sulfate\text{-}sulfide}$ on $[SO_4^{2-}]_{aq}$ yields a linear strong positive relationship with a strong positive correlation (r^2 = +0.980, $p(\alpha) < 0.01$). The trend represents an increase in $\Delta^{34}S_{sulfate\text{-}sulfide}$ from ~4-6‰ at 0.1 mM to ~30-60‰ at 29 mM (i.e., modern seawater $[SO_4^{2-}]$). $\Delta^{34}S_{sulfate\text{-}sulfide}$ appears to peak at $[SO_4^{2-}]_{aq}$ of 15-20 mM, with a mean value ~5-10‰ greater than for $[SO_4^{2-}]_{aq}$ of 29 mM $[SO_4^{2-}]_{SW}$, but this effect is small relative to the overall relationship between $\Delta^{34}S_{sulfate\text{-}sulfide}$ and $[SO_4^{2-}]_{aq}$, and we did not factor it separately into the regression analysis. For hypersaline environments in which $[SO_4^{2-}]_{aq}$ >29 mM, $\Delta^{34}S_{sulfate\text{-}sulfide}$ does not continue to rise but, rather, shows roughly the same range as for modern seawater (Fig. 2a). Finally, we analyzed the data by redox environment and found only minor and statistically insignificant differences between oxic and euxinic settings (n.b., hypersaline environments were not included in this analysis). The distributions of the oxic and euxinic datasets show broad overlap (Fig. 2a), so benthic redox conditions appear to exhibit no discernible influence on the relationship of $\Delta^{34}S_{sulfate\text{-}sulfide}$ to $[SO_4^{2-}]_{aq}$.

Our analysis demonstrates that a strong relationship exists between F_{MSR} and $[SO_4^{2-}]_{aq}$ in natural aqueous systems (r^2 = +0.980, $p(\alpha) < 0.01$; Fig. 2a). Our results are similar to, although more linear and more statistically robust than, those reported by Habicht et al. (2002) on the basis of culture experiments. We recognize that there are multiple environmental and physiological controls on fractionation by sulfate reducers (see discussion belowSection 3), and that under certain natural and experimental conditions the relationship of F_{MSR} to $[SO_4^{2-}]_{aq}$ can deviate markedly from that in our dataset. However, the pattern of covariation between F_{MSR} and $[SO_4^{2-}]_{aq}$ documented here represents a robust relationship that appears to hold for a wide

Formatted: Space Before: 0 pt, Don't adjust space between Latin and Asian text, Don't adjust space between Asian text and numbers

Formatted: Space After: 6 pt, Don't adjust space between Latin and Asian text, Don't adjust space between Asian text and numbers

Formatted: Space After: 6 pt

Formatted: Font: Italic

Formatted: Font: Symbol

Formatted: Space Before: 6 pt, Don't adjust space between Latin and Asian text, Don't adjust space between Asian text and numbers

Formatted: Font: Italic

Formatted: Font: Symbol

range of natural environments, reflecting ~~a~~ the ~~widespread and~~ possibly near-ubiquitous influence of $[SO_4^{2-}]_{aq}$ on F_{MSR}. ~~The apparent breakdown of this relationship in hypersaline environments (Fig. 2a) needs further testing; our dataset for hypersaline environments is too small (n = 6) to reach firm conclusions.~~ ~~Nonetheless, t~~However, the strength of the F_{MSR}-$[SO_4^{2-}]_{aq}$ relationship ~~shown in Figure 2a~~for watermasses with salinities ranging up to ~40 psu suggests that it can serve as a basis for evaluating the $[SO_4^{2-}]_{aq}$ of ancient seawater. Seawater $[SO_4^{2-}]$ can be estimated graphically by projecting measured values of $\Delta^{34}S_{CAS\text{-}PY}$ from the ordinal scale to the MSR trend and then to the abscissa (Fig. 2b), or by using the following empirical equation:

$$\log[SO_4^{2-}] = ~~0.42 \times~~ (\log(\Delta^{34}S_{CAS\text{-}PY}) - 1.10) / 0.42 ~~- 0.15~~ \quad (6)$$

The upper and lower uncertainty limits for estimates of seawater $[SO_4^{2-}]$ based on this relationship are:

$$\log[SO_4^{2-}] = ~~0.40 \times~~ (\log(\Delta^{34}S_{CAS\text{-}PY}) - 1.18) / 0.40 ~~- 0.02~~ \quad \text{(upper limit)} \quad (7)$$

$$\log[SO_4^{2-}] = ~~0.44 \times~~ (\log(\Delta^{34}S_{CAS\text{-}PY}) - 1.02) / 0.44 ~~- 0.28~~ \quad \text{(lower limit)} \quad (8)$$

In order to account for uncertainties in $\Delta^{34}S_{CAS\text{-}PY}$ as well as the F_{MSR} regression, estimates of minimum $[SO_4^{2-}]_{SW}$ should make use of minimum $\Delta^{34}S_{CAS\text{-}PY}$ values in combination with the upper uncertainty limit equation (Eq. 7), and estimates of maximum $[SO_4^{2-}]_{SW}$ should make use of maximum $\Delta^{34}S_{CAS\text{-}PY}$ values in combination with the lower uncertainty limit equation (Eq. 8; Fig. 2b).

3 Controls on fractionation by microbial sulfate reducers

The biogeochemical nature of the microbial sulfate reduction (MSR) process and its associated S-isotope fractionations have been extensively investigated in earlier studies. Sulfate reducers preferentially utilize sulfate containing ^{32}S during dissimilatory reduction to hydrogen sulfide in conjunction with the anaerobic decay of organic matter (Kaplan, 1983; Canfield, 2001; Bradley et al., 2011). The exact controls on this isotopic discrimination continue to be a topic of intense debate. The paradigmatic view is that this fractionation is mainly a kinetic effect associated with the rate-limiting step for intracellular sulfate processing, although it is known that fractionation also may accompany sulfate transport across the cell membrane (Rees, 1973; Detmers et al., 2001; Brüchert, 2004; Bradley et al., 2011). The kinetic effect is thought to be dependent on aqueous sulfate concentrations, with substantially larger fractionations associated with $[SO_4^{2-}]_{aq}$ >~200 μM (Habicht et al., 2002; Gomes and Hurtgen, 2013; but see Canfield, 2001, for a counter example). Rees (1973) proposed a maximum discrimination of 46‰ but the theoretical basis for this value was re-assessed by Brunner and Bernasconi (2005). Recent studies have documented F_{MSR} as large as 66‰ in culture experiments (Sim et al., 2011a) and 70-80~~2~~‰ in natural systems (Rudnicki et al., 2001; Wortmann et al., 2001; Canfield et al., 2010). Even larger fractionations have been reported but are generally considered to be

Formatted: Font color: Auto

Formatted: Font color: Auto

Formatted: Space After: 6 pt

the result of multistage disproportionation of intermediate-oxidation-state sulfur compounds (Canfield and Thamdrup, 1994).

Investigations of natural and experimental systems have documented a number of additional controls on F_{MSR}. One of the most important controls is f_{SO4}, i.e., the fraction of remaining dissolved sulfate (Gomes and Hurtgen, 2013). In 'open systems' containing a high concentration of dissolved sulfate (e.g., the modern ocean), f_{SO4} does not vary measurably from 1.0 because the quantity of sulfate converted to sulfide via MSR is a small fraction of the total aqueous sulfate inventory. In this case, the produced sulfide will show the maximum degree of fractionation, which is typically ~30 to 60‰ in modern marine systems (~~Habicht and Canfield, 1997;~~ Fig. 2a; Table A1). In contrast, in 'closed systems' in which the aqueous sulfate inventory is limited (e.g., sediment porewaters or low-sulfate freshwater systems), dissolved sulfate concentrations can be substantially reduced or completely depleted through MSR, causing f_{SO4} to evolve toward zero. As $[SO_4^{2-}]_{aq}$ becomes smaller, sulfate reducers utilize a progressively larger fraction of the total dissolved sulfate pool, reducing the effective fractionation to small values (Habicht et al., 2002; Gomes and Hurtgen, 2013). In these settings, the aggregate $\delta^{34}S$ composition of the produced sulfide approaches that of the original aqueous sulfate inventory, and $\Delta^{34}S_{sulfate\text{-}sulfide}$ approaches zero (Kaplan, 1983; Habicht et al., 2002). In a macro sense, f_{SO4} can be proxied by $[SO_4^{2-}]_{aq}$, accounting for the strong first-order relationship between the latter parameter and $\Delta^{34}S_{sulfate\text{-}sulfide}$ (~~r^2~~ = ~~+~~0.9~~8~~0, $p(\alpha) < 0.01$; Fig. 2a). However, not all researchers agree on the importance of f_{SO4} as a control on F_{MSR} (e.g., Leavitt et al., 2013).

Other factors may influence F_{MSR} under certain conditions. First, different dissimilatory reduction pathways yield different isotopic discriminations. Oxidation of organic substrates to CO_2 yields larger fractionations (~30-60‰) than oxidation to acetate (<18‰) (Detmers et al., 2001; Brüchert et al., 2001; Brüchert, 2004). Incomplete oxidation of organic substrates is a feature characteristic of sulfate reducers in hypersaline environments (Habicht and Canfield, 1997; Oren, 1999; Detmers et al., 2001; Stam et al., 2010) and may account for the somewhat smaller fractionations typically encountered in such environments (Fig. 2a). Second, the type of organic substrate also matters, as ethanol, lactate, glucose, and other compounds yield~~ed a range~~different ~~of~~ fractionations under otherwise similar conditions (Canfield, 2001; Detmers et al., 2001; Kleikemper et al., 2004; Sim et al., 2011b). Third, sulfate reduction rates may also influence F_{MSR}, with higher rates associated with smaller isotopic discriminations (Kaplan and Rittenberg, 1964; Kemp and Thode, 1968; Rees, 1973; Chambers et al., 1975; Habicht and Canfield, 1996; Brüchert et al., 2001; Canfield, 2001; Brunner and Bernasconi, 2005). Recent experiments by Leavitt et al. (2013) showed that F_{MSR} declines rapidly with increasing sulfate reduction rates before leveling off at ~15-20‰ at rates >50 mmol H_2S per unit substrate per day. Habicht and Canfield (2001) hypothesized that F_{MSR} is only incidentally related to sulfate reduction rates because both are correlated with the disproportionation of intermediate-oxidation-state S compounds by sulfur-oxidizing bacteria, which have probably been present since the Archean (Johnston et al., 2005; Wacey et al., 2010). Fourth, cell external sulfide (CES) concentrations, when high, can cause back-diffusion of sulfide into cells, with subsequent oxidative recycling to sulfate (Brunner and Bernasconi, 2005; Eckert et al., 2011). Finally, temperature has been shown to affect F_{MSR} in some studies (e.g., Canfield et al., 2006) but not

others (e.g., Detmers et al., 2001). The influence of temperature on F_{MSR} may operate through the species-specific temperature dependence of enzymes.

Research to date clearly shows that controls on microbial sulfate reduction are complex and incompletely understood. This situation reflects the diverse composition of the microbial communities that process sulfur in the marine environment and the range of isotopic fractionations associated with those processes (Brüchert, 2004). Yet even though multiple environmental and physiological factors influence F_{MSR}, the strength of its relationship to $[SO_4^{2-}]_{aq}$, as documented in this study (Fig. 2a), implies that aqueous sulfate concentrations are the dominant first-order control on F_{MSR}, and that other factors such as organic substrate, rates of MSR, and temperature are second-order controls whose effects may be randomized at a larger scale and do not obscure the dominant influence of $[SO_4^{2-}]_{aq}$ in most environments. Whether the quantitative form of our F_{MSR}-$[SO_4^{2-}]_{aq}$ relationship is unique to the present or valid for the geologic past is unclear. Microbial S-cycling processes are thought to have been conservative through time (e.g., Wacey et al., 2010), although lower atmospheric pO_2 prior to ~635 Ma~~0.63 Ga~~ may have limited disproportionation of intermediate-oxidation-state sulfur compounds and, thus, the potential for large fractionations (Habicht and Canfield, 2001; Sørensen and Canfield, 2004; Johnston et al., 2005). In the following analysis, we adopt the F_{MSR}-$[SO_4^{2-}]_{aq}$ relationship of Figure 2a as a basis for evaluating the $[SO_4^{2-}]_{aq}$ of ancient seawater from ~~≈~~635 Ma~~0.63 Ga~~ to the present.

4. Estimation of seawater sulfate concentrations since ~~630~~ 635 Ma

4.1 General considerations and modeling protocol

~~T~~The rate and MSR-trend methods ~~of estimating $[SO_4^{2-}]_{SW}$ provide a basis for~~can be applied to analysis of long-term variation in seawater sulfate concentrations. Although both methods utilize measured values of $\Delta^{34}S_{sulfate\text{-}sulfide}$ as a proxy for F_{MSR}, they are quasi-independent in having different transform functions. The transform function of the rate method (Eqs. 3-4) makes use of observed rates of seawater sulfate S-isotopic variation (i.e., $\partial\delta^{34}S_{CAS}/\partial t(max)$), whereas that of the MSR-trend method (Eqs. 6-8) makes use of an empirical relationship between F_{MSR} and $[SO_4^{2-}]_{aq}$. The two methods ~~appear to be~~are applicable over approximately the same range of $[SO_4^{2-}]_{SW}$ concentrations (~0.1-30 mM). However, their transform functions have different sensitivities to $[SO_4^{2-}]_{SW}$, with that of the MSR-trend method being greater ~~owing to~~as reflected in its lower slope (m = 0.42; Fig. 2) compared with that of the rate method (m = 1.0; Fig. 1). Thus, a combination of ~~both~~ the two methods may be the most useful approach to constraining ancient seawater $[SO_4^{2-}]$. Because the rate method yields estimates of *maximum* likely $[SO_4^{2-}]_{SW}$, it should generally yield a higher estimated sulfate concentration than the MSR-trend method, which estimates the mean $[SO_4^{2-}]_{SW}$ of the time interval of interest. The pairing of these procedures is thus useful in providing both mean and maximum estimates of paleo-seawater sulfate concentrations. Combining these two methods is also useful in providing a check on the robustness of the results. For example, if the maximum estimate yielded by the rate method is less than the mean estimate yielded by the MSR-trend method, then the results should be considered unreliable.

Formatted: Space After: 6 pt

Both the rate and MSR-trend methods require defined input variables for calculation of paleo-seawater [SO_4^{2-}]. For the rate method, a record of secular variation in seawater sulfate $\delta^{34}S$ is needed from which to calculate $\partial\delta^{34}S_{CAS}/\partial t$. We generated a seawater sulfate $\delta^{34}S$ record for the Phanerozoic by combining published $\delta^{34}S_{CAS}$ datasets for the Cenozoic (Paytan et al., 1998), Cretaceous (Paytan et al., 2004), and pre-Cretaceous (Kampschulte and Strauss, 2004) (Table A2; Fig. 3a). We calculated LOWESS curves for this composite record per the methodology of Song et al. (2014). LOWESS curves were generated at both a low frequency (i.e., 5-Myr steps) and a high frequency (i.e., 1-Myr steps), the latter resulting in less smoothing of the long-term $\delta^{34}S_{CAS}$ trend (Fig. 3a). The LOWESS curves were then used to calculate rates of change in seawater sulfate concentrations ($\partial\delta^{34}S_{SO4}/\partial t$) through the Phanerozoic (Fig. 3b). For both the rate and MSR-trend methods, $\Delta^{34}S_{sulfate\text{-}sulfide}$ is a defined input variable. As a proxy, we utilized the Phanerozoic $\Delta^{34}S_{CAS\text{-}PY}$ record of Wu et al. (2010). According to this record, $\Delta^{34}S_{CAS\text{-}PY}$ averaged 30±3‰ from 540 to 300 Ma, increased gradually from 30‰ to 45‰ between 300 and 270 Ma, and then fluctuated around 42±5‰ from 270 to 0 Ma (Fig. 3c).

4.2 Long-term variation in seawater sulfate concentrations

Our composite record shows that seawater sulfate $\delta^{34}S$ was heavy (~30-40‰) during the Ediacaran to Middle Cambrian, ~~then~~ declined steeply during the Late Cambrian to Early Ordovician, and stabilized at intermediate values (~20-30‰) during the Middle Ordovician to Early Devonian (Table A3; Fig. 3a). Sulfate $\delta^{34}S$ declined further during the Middle Devonian to Early Mississippian, reaching a minimum of ~12-16‰ during the mid-Mississippian to end-Permian. Sulfate $\delta^{34}S$ then rose sharply to ~20‰ during the Early Triassic, before declining slightly to a local minimum of ~15‰ around the Jurassic-Cretaceous boundary. Sulfate $\delta^{34}S$ rose slowly during the Cretaceous and early Cenozoic, ~~finishing with a rapid i~~increased rapidly from 17‰ to 22‰ at 40-50 Ma, ~~before~~ and then stabilized~~ing~~ at 21-23‰ during the mid- to late Cenozoic (Fig. 3a). The low-frequency LOWESS curve exhibits low rates of $\delta^{34}S$ variation, with a mean of 0.25(±0.17)‰ Myr^{-1} and a maximum of ~0.8‰ Myr^{-1} (Fig. 3b). The high-frequency LOWESS curve exhibits somewhat higher rates of $\delta^{34}S$ variation, with a mean of 0.40(±0.45)‰ Myr^{-1} and a maximum of ~2.5‰ Myr^{-1} (Fig. 3b). Both curves show exceptionally low rates of seawater sulfate $\delta^{34}S$ variation during the Late Cretaceous and Cenozoic (the 'Cenozoic minimum') and the mid-Mississippian to mid-Permian (the 'Late Paleozoic minimum') ~~and substantially higher rates during other intervals~~.

Our reconstructions of mean and maximum seawater sulfate concentrations through the Phanerozoic, based respectively on the MSR-trend and rate methods, are shown in Figure 4. The mean curve suggests that $[SO_4^{2-}]_{SW}$ was low in the late Ediacaran (~1-4 mM) but rose sharply in the Early Cambrian (to ~3-15 mM) and remained in that range until the Permian. A long, slow rise in $[SO_4^{2-}]_{SW}$ began in the Early Permian and culminated at ~12-38 mM in the Middle Triassic. Subsequently, $[SO_4^{2-}]_{SW}$ declined slightly ~~until~~ by the mid-Cretaceous (to ~7-25 mM) ~~(to ~7-25 mM)~~ and then rose slightly during the Late Cretaceous to early Cenozoic (to 11-35 mM). The standard deviation range for the mean curve (blue band) suggests an uncertainty of plus or minus a factor of ~2×~~X~~ in the mean estimate, with the magnitude of the uncertainty

Formatted: Space After: 6 pt

shrinking modestly from the Cambrian to the present. The modern seawater sulfate concentration of 29 mM falls within the standard deviation range of the mean trend (Fig. 4).

A maximum $[SO_4^{2-}]_{SW}$ curve can be calculated for both the low- and high-frequency Phanerozoic $\delta^{34}S$ records of Figure 3a. The low- and high-frequency maximum $[SO_4^{2-}]_{SW}$ curves (shown as black and red lines, respectively, in Figure 4) mirror the upward trend through the Phanerozoic seen in the mean curve and, thus, are consistent with a factor of ~4~~x~~X increase in seawater sulfate concentrations since the Early Cambrian. Although the maximum $[SO_4^{2-}]_{SW}$ curves exhibit values that are mostly unrealistically large, it is worth noting that (1) these curves represent the maximum possible, not the most likely, concentrations of seawater sulfate; and (2) the smallest values on the maximum curves are more robust constraints on $[SO_4^{2-}]_{SW}$ than the largest values. The second observation is based on the fact that the smallest values derive from the largest measured rates of $\delta^{34}S_{CAS}$ variation (Fig. 3b), i.e., those rates than most closely approach the theoretical maximum, whereas the largest values are associated with intervals of little or no $\delta^{34}S_{CAS}$ variation. Thus, the lower envelope of maximum $[SO_4^{2-}]_{SW}$ values (dashed line, Fig. 4) provides a more useful constraint on seawater sulfate concentrations than the full curve~~.~~. We also suggest that, although the upper limits on $[SO_4^{2-}]_{SW}$ imposed by the rate method may have limited utility for assessment of Phanerozoic seawater sulfate, this method may be of greater value in analyzing Archean and Proterozoic seawater sulfate concentrations, which are thought to have been quite low (<1 mM; Kah et al., 2004; Canfield et al., 2007; Planavsky et al., 2012).

The results of the rate method are dependent on several factors that influence the estimation of rates of seawater sulfate $\delta^{34}S$ variation. ~~On the one hand,~~ $\partial\delta^{34}S_{SO4}/\partial t(max)$ ~~can~~ may be overestimated if there is an increase in $\delta^{34}S_{CAS}$ variance due to diagenesis ~~of samples~~ or procedural artifacts during CAS extraction, or it may be ~~. On the other hand,~~underestimated if there is a decrease in $\delta^{34}S_{CAS}$ variance due to diagenesis or procedural ~~-~~data smoothing. Data smoothing ~~is~~is ~~-~~inherent in the calculation of LOWESS curves ~~calculation, reducing the variance in high-frequency datasets~~ (cf. Song et al., 2014), and ~~thus resulting in an~~ underestimation of $\partial\delta^{34}S_{SO4}/\partial t(max)$ is thus almost certain when smoothed $\delta^{34}S_{SO4}$ datasets are used as inputs. ~~The conclusion that such s~~It~~moothing has occurred in generating~~may be responsible for the absence of short-term excursions in ~~the~~ our Phanerozoic $[SO_4^{2-}]_{SW}$ ~~LOWESS~~ curve ~~of~~ (Fig. ~~ure~~ 3a) ~~is inescapable~~ , since ~~given the documented existence of a number of short~~a number of short (~~(~~<2 ~~-~~Myr) intervals ~~) intervals~~ of strongly elevated $\partial\delta^{34}S_{SO4}/\partial t$ rates ~~within~~ have been documented for the Phanerozoic (Wortmann and Chernyavsky, 2007; Adams et al., 2010; Gill et al., 2011a,b; Newton et al., 2011; Wotte et al., 2012; Owens et al., 2013; Song et al., 2014; see ~~below for further analysis~~Section 4.3). During these intervals, $\partial\delta^{34}S_{SO4}/\partial t$ ranged from 10 to >50‰ Myr^{-1} (Table A4), rates that are considerably higher than peak rates for the long-term $\delta^{34}S_{CAS}$ curve (ca. 2-4‰ Myr^{-1}; Fig. 3b). Because lower values for $\partial\delta^{34}S_{SO4}/\partial t(max)$ yield higher maximum estimates of $[SO_4^{2-}]$ for ancient seawater (Eqs. 3-4), smoothing may account for some of the divergence between the mean and maximum trends in Figure 4. The existence of such ~~Phanerozoic appears to be characterized by such~~ short-term episodes of seawater sulfate drawdown during the Phanerozoic has been attributed to several causes, including~~, mainly as a consequence of~~ episodic massive evaporite deposition (Wortmann and Paytan, 2012) and

reduced~~. However, other factors may have contributed to transient changes in the seawater sulfate inventory, e.g., reduced~~ ventilation of marine sediments and a consequent increase in MSR in the aftermath of mass extinction events (Canfield and Farquhar, 2009).

Comparison of our Phanerozoic seawater sulfate concentration curve with previously published estimates reveals similarities and differences (Fig. 5). Most of these records exhibit a local minimum during the Jurassic or Cretaceous, although the absolute estimates of [SO_4^{2-}] for this minimum vary widely (~2 to 25 mM~~); our value of 13 mM is close to the median estimate of ~10 mM~~). Our higher estimates (~13-16 mM) compared to those of Wortmann and Paytan (2012) (uniformly <7 mM) may be a consequence of our choice of input dataset, i.e., the Phanerozoic $\Delta^{34}S_{CAS\text{-}PY}$ record of Wu et al. (2010). The latter is based on a large compilative dataset that yielded a strongly time-averaged trend, which is likely to have dampened variation in our $[SO_4^{2-}]_{SW}$ estimates. The various records are also in agreement that seawater sulfate was elevated during the Permian-Triassic, with concentrations of ~15-30 mM. The records diverge prior to the Permian, however, with one model (Holser et al., 1989) suggesting high values (30-50 mM) and another model (Berner, 2004) low values (<2 mM) through the mid-Paleozoic. Our model indicates intermediate sulfate concentrations (5-10 mM) at that time (Fig. 5). The various records also show dissimilar patterns across the Ediacaran-Cambrian boundary, with uniformly high values in the Holser et al. (1989) model and steeply falling values in the Berner (2004) model. The results of the present study favor a steep rise in seawater sulfate at this boundary~~ (see next section for further analysis)~~. Our Phanerozoic seawater sulfate concentration record, along with that of Halevy et al. (2012), is in good agreement with the available fluid-inclusion data (Fig. 5) and, thus, appears generally robust, although it probably does not capture short-term episodes of seawater sulfate drawdown (~~cf. Wortmann and Paytan, 2012~~see Section 4.3).

Our reconstruction of long-term secular variation in seawater sulfate concentrations shows a strong relationship to first-order Phanerozoic climate cycles (cf. Algeo et al., ~~2013~~2014). In particular, the interval of the Late Paleozoic Ice Age, which lasted from the mid-Mississippian through the mid-Permian, was characterized by a major change in the oceanic sulfate reservoir. At that time, minimum values developed for both seawater sulfate $\delta^{34}S$ (~12-16‰; Fig. 3a) and rates of $\delta^{34}S_{SO4}$ variation (<1‰ Myr^{-1}; Fig. 3b), accompanied by a concurrent increase in ~~mean~~ sulfate-sulfide fractionation (from <30‰ to >40‰; Fig. 3c). Whether these are general features of seawater sulfate during icehouse climate modes is not entirely certain. A second interval of ~~major~~global climatic cooling and continental glaciation during the Late Cretaceous and Cenozoic also shows low rates of $\delta^{34}S_{SO4}$ variation and an increase in sulfate-sulfide fractionation but, in contrast to the Late Paleozoic, ^{34}S-enriched and relatively stable seawater sulfate $\delta^{34}S$ values (Fig. 3). The greater stability of seawater sulfate $\delta^{34}S$ during the Cenozoic relative to the Late Paleozoic may be due to a long-term increase in total seawater sulfate mass (Figs. 4-5). We hypothesize that the Late Paleozoic was characterized by low rates of pyrite burial (hence, lower $\delta^{34}S_{SO4}$) and a consequent increase in the mass of seawater sulfate (hence, lower $\partial\delta^{34}S_{SO4}/\partial t$) (cf. Halevy et al., 2012). Low rates of pyrite burial at that time may have been due to a combination of lower sea-level elevations (reducing the total shelf area available for sulfate reduction; cf. Halevy et al., 2012; Algeo et al., 2014), enhanced oceanic ventilation (increasing aerobic decay of organic matter), and increased burial of organic

Formatted: Space After: 6 pt, Don't adjust space between Latin and Asian text, Don't adjust space between Asian text and numbers

Formatted: Font color: Auto

Formatted: Font color: Auto

Formatted: Font color: Auto

Formatted: Font color: Auto

Formatted: Font color: Auto

Formatted: Font color: Auto

Formatted: Font color: Auto

Formatted: Font color: Auto

Formatted: Font color: Auto

Formatted: Font color: Auto

Formatted: Font color: Auto

Formatted: Font color: Auto

Formatted: Space After: 6 pt

matter in low-sulfate freshwater settings, which was linked to the spread of terrestrial floras (DiMichele and Hook, 1992).

4.3 High-frequency variation in seawater sulfate during the Neoproterozoic and Phanerozoic

We applied the rate and MSR-trend methods to an analysis of short-term variation in $[SO_4^{2-}]_{SW}$ during selected intervals of the Neoproterozoic and Phanerozoic for which high-resolution $\delta^{34}S_{CAS}$ studies are available. For the Neoproterozoic, recent studies have provided S-isotope records from a number of sites globally as well as improved radiometric geochronologic constraints that are needed for the rate method. Based on these studies, we have estimated $\partial\delta^{34}S_{SO4}/\partial t(max)$ for 10 late Neoproterozoic units (Table A4; Fig. 6). Radiometric studies of the Doushantuo Formation in South China (Halverson et al., 2005; Zhang et al., 2005, 2008) provided key ages from which we calculated $\partial\delta^{34}S_{CAS}/\partial t(max)$ of 5‰ Myr^{-1} at ~636-633 Ma and 1.3‰ Myr^{-1} at ~568-551 Ma (McFadden et al., 2008; Li et al., 2010). The Neoproterozoic succession of Sonora, Mexico yielded $\partial\delta^{34}S_{CAS}/\partial t(max)$ estimates of 6‰ Myr^{-1} and 4‰ Myr^{-1} (Loyd et al., 2012, 2013). The latest Neoproterozic Zarls Formation (Nama Group) in Namibia and upper Huqf Supergroup in Oman yielded $\partial\delta^{34}S_{CAS}/\partial t(max)$ estimates of 20‰ Myr^{-1} and 40‰ Myr^{-1}, respectively, at 549-547 Ma (Fike and Grotzinger, 2008; Ries et al., 2009). The rate method yielded $[SO_4^{2-}]_{SW}$ estimates ranging from <0.1 to >100 mM, ~~although~~ with ~~the majority fell~~most between ~1 and 10 mM (Table A4). The MSR-trend method yielded $[SO_4^{2-}]_{SW}$ estimates ranging from <0.1 to 70 mM, with ~~a majority~~most between ~1 and 16 mM. Many~~ost~~ units exhibit combinations of $\partial\delta^{34}S_{CAS}/\partial t(max)$ and $\Delta^{34}S_{CAS\text{-}PY}$ values that plot close to or slightly below the MSR trend (Fig. 6), yielding $[SO_4^{2-}]_{SW}$ estimates for the MSR-trend method that are equal to or somewhat smaller than the rate-based estimates. This pattern conforms to our expectation that the rate method yields maximum estimates of $[SO_4^{2-}]_{SW}$. The only potentially anomalous result is for the upper Huqf Supergroup, which yielded a ~~'mean' estimate based on the~~ MSR-trend ~~method~~ estimate (12-45 mM) that is larger than the ~~'maximum' estimate based on the~~ rate ~~method~~ estimate (1.5-8 mM; Table A4).

We also analyzed $[SO_4^{2-}]_{SW}$ for a set of 8 units of Cambrian age. These units yielded $\partial\delta^{34}S_{CAS}/\partial t(max)$ of 7 to 23‰ Myr^{-1} for the Early Cambrian, 9 to 20‰ Myr^{-1} for the Early-Middle Cambrian boundary (EMCB), and 8 to 20‰ Myr^{-1} for the Late Cambrian SPICE (Table A4; Fig. 7). These ranges are sufficiently similar that they suggest a limited range of seawater $[SO_4^{2-}]$ variation during the Cambrian. The rate method yielded $[SO_4^{2-}]_{SW}$ estimates ranging from <0.1 to 18 mM, ~~although the majority fell~~with most between ~1 and 6 mM. The MSR-trend method yielded $[SO_4^{2-}]_{SW}$ estimates ranging from <0.1 to 40 mM, with ~~a majority~~most between ~1 and 8 mM. The two methods thus yielded similar estimates of seawater sulfate concentrations, implying that the results are reasonably robust and that the rate method is not yielding unrealistically large values. All Cambrian units show~~ed~~ sulfate-sulfide fractionations smaller than the Paleozoic mean of 30±5 (Wu et al., 2010), resulting in lower $[SO_4^{2-}]_{SW}$ estimates than for the long-term record (Fig. 4). Once again, most units exhibit combinations of $\partial\delta^{34}S_{CAS}/\partial t(max)$ and $\Delta^{34}S_{CAS\text{-}PY}$ values that plot close to or slightly below the MSR trend (Fig. 7). However, two units (the SPICE events in Australia and Nevada) yield~~ed 'mean' estimates based~~

Formatted: Space Before: 0 pt

Formatted: Space After: 6 pt

~~on the~~ MSR-trend ~~method~~ estimates that are larger than ~~their 'maximum' estimates based on~~ their rate~~-~~method estimates. The reasons for these potentially anomalous results will be considered below.

Finally, we analyzed a set of 8 Mesozoic units, ranging in age from the Early Triassic to the late Middle Cretaceous (Table A4; Fig. 8). These units ~~yielded~~ show $\partial\delta^{34}S_{CAS}/\partial t(max)$ of 6 to 60‰ Myr^{-1}, with the highest rates during the Early Triassic and Early Jurassic. The rate method yielded $[SO_4^{2-}]_{SW}$ estimates ranging from 1.1 to 120 mM, ~~although the majority fell~~with most between ~3 and 20 mM. The MSR-trend method yielded $[SO_4^{2-}]_{SW}$ estimates ranging from 1 to 110 mM, with ~~a majority~~most between ~30 and 100 mM (Table A4). In contrast to the late Neoproterozoic and Cambrian ~~(see above)~~, many~~ost~~ Mesozoic units exhibit a narrow spread of $\Delta^{34}S_{CAS\text{-}PY}$ values that conform with the mean sulfate-sulfide fractionation for the Mesozoic-Cenozoic (Wu et al., 2010; Fig. 8) and that are within the range ~~of values shown by~~for modern marine systems (~30-60‰; Table A1~~Habicht and Canfield, 1997~~). As a consequence, ~~the majority of~~many Mesozoic units exhibit the anomalous pattern of having ~~'mean' estimates based on the~~ MSR-trend ~~method~~ estimates that are larger than their ~~'maximum' estimates based on the~~ rate~~-~~method estimates~~(Fig. 8)~~.

Ideally, the rate and MSR-trend methods will yield similar $[SO_4^{2-}]_{SW}$ estimates, providing support for the correctness of the results, and a majority of the paleomarine units considered in this study follow this pattern. However, ~~, but differing estimates may also provide information. Although this is true of the majority of the units above, a~~a subset of the study units show ~~deviations~~ differences that fall into two categories: (1) Type I deviation: rate method estimates >> MSR-trend estimates ~~units with unusually low $\partial\delta^{34}S_{CAS}/\partial t(max)$, yielding rate-based estimates of $[SO_4^{2-}]_{SW}$ much larger than MSR-trend-based estimates~~ (lower right field, Fig. 9), and (2) Type II deviation: MSR-trend estimates >> rate method estimates ~~units with unusually high $\partial\delta^{34}S_{CAS}/\partial t(max)$, yielding rate-based estimates of $[SO_4^{2-}]_{SW}$ much smaller than MSR-trend-based estimates~~ (upper left field, Fig. 9). Such deviations may provide insights into underlying controls on seawater sulfate concentrations. The most likely explanation for the ~~first type of~~ Type I deviations is that the ~~observed~~ measured $\partial\delta^{34}S_{CAS}/\partial t(max)$ for a given unit is much less than its theoretical maximum. This situation can develop whenever the marine sulfur cycle is in equilibrium (i.e., source and sink fluxes in balance), reflecting persistently stable environmental conditions. In this case, the rate-method~~based~~ estimate of $[SO_4^{2-}]_{SW}$ would have little relationship to actual $[SO_4^{2-}]_{SW}$, although the MSR-trend ~~-based~~ estimate may still be a good proxy for $[SO_4^{2-}]_{SW}$. Surprisingly, very few of the analyzed units (Table A4) show ~~a significant~~Type I deviations ~~of this type~~, perhaps because the most heavily scrutinized ancient geologic epochs are those with unstable environments.

~~The second type of~~Type II deviations, in which $\partial\delta^{34}S_{CAS}/\partial t(max)$ is anomalously high, are~~is~~ more common, being present in three units of late Neoproterozoic and Cambrian age (Figs. 6-7) and ~~no fewer than~~ 7 out of 8 units of Mesozoic age (Fig. 8). ~~This pattern does not have a single obvious explanation (as for the first deviation type), and several potential causes warrant consideration~~Several factors might potentially produce this pattern. First, $\partial\delta^{34}S_{CAS}/\partial t(max)$ may have been overestimated ~~because of problems related to dating~~

~~inaccuracies~~owing to inadequate geochronologic constraints, diagenetic artifacts, or analytical uncertainties in measuring $\delta^{34}S_{CAS}$. However, the ~~observation~~ fact that ~~deviations of this type~~Type II deviations are more common among Mesozoic units (Fig. 8), which are generally better dated and less diagenetically altered than older units (Figs. 6-7), suggests that such problems are relatively uncommon and unlikely to be responsible for most ~~of the observed~~such anomalies. Second, the measured $\Delta^{34}S_{CAS\text{-}PY}$ for a given paleomarine unit may be unrepresentative, perhaps because of unusually large MSR fractionation~~s during MSR~~ (cf. Habicht et al., 2002; Canfield et al., 2010). This explanation may be applicable, for example, to ~~the~~ Pleistocene Mediterranean sapropel~~s of (~~Scheiderich et al., ~~(~~2010), which exhibit~~s an~~ unusually large $\Delta^{34}S_{CAS\text{-}PY}$ values (60±5‰; Fig. 8). However, none of the anomalous units of late Neoproterozoic, Cambrian, or Mesozoic age exhibits a $\Delta^{34}S_{CAS\text{-}PY}$ larger than the typical modern range of ~30-60‰, so elevated sulfate-sulfide fractionation is unlikely as a general explanation. We are therefore inclined to regard most ~~these~~ Type II deviations as products of local depositional conditions and to seek an environmentally based mechanism to account for them.

~~One method of generating~~A possible environmental explanation for Type II~~the second type of~~ deviation~~s~~ is~~is for~~ sulfate reduction with~~to occur~~ in a restricted-marine basin. In this case, $\Delta^{34}S_{CAS\text{-}PY}$ ~~will be~~is controlled by seawater $[SO_4^{2-}]$, which may be identical (or nearly so) to that in the global ocean. However, the total mass of sulfate in ~~a~~ the restricted-marine basin will be much less than that in the global ocean, allowing a more rapid evolution of seawater sulfate $\delta^{34}S$ in response to oceanographic perturbations. We hypothesize that most of the ~~r all of the type two~~Type II deviations in our study units are the product of MSR within semi-restricted marine basins. For example, t~~T~~he Neoproterozoic Ara Group (Huqf Supergroup) of Oman was deposited in a fault-bounded basin in which massive evaporite deposits accumulated (Fike and Grotzinger, 2008). Also, m~~M~~ost of the Mesozoic units showing ~~type two~~Type II deviations are ~~also~~ known to have been deposited in basins that were ~~exhibiting~~ subject to ~~some~~ a degree of watermass restriction. The Triassic-Jurassic European epicontinental sea was broad, shallow, and laced with local tectonic grabens with restricted deepwater circulation (Röhl et al., 2001; Berra et al., 2010). The Early Cretaceous South Atlantic was only weakly connected to the global ocean during deposition of Aptian ~~(Early Cretaceous)~~ sediments (Wortmann and Chernyavsky, 2007), and restriction of the Atlantic Ocean continued at least through deposition of organic-rich facies at the Cenomanian-Turonian boundary (Owens et al., 2013). The Cretaceous Western Interior Seaway was almost certainly semi-restricted throughout its existence (Adams et al., 2010). The only Mesozoic unit not to show a ~~type two~~Type II deviation, the Middle Triassic Bravaisberget Formation of Spitsbergen (Karcz, 2010; Fig. 8), was deposited in the largely unrestricted Boreal Ocean. These examples serve to illustrate the need to understand the hydrography of paleomarine basins in applying the rate method of estimating paleoseawater sulfate concentrations.

Comparison of the $[SO_4^{2-}]_{SW}$ estimates for individual Neoproterozoic and Phanerozoic units shown in Figures 6-8 with the long-term $[SO_4^{2-}]_{SW}$ curve in Figure 4 provides additional insights regarding ~~the history of~~secular variation in seawater sulfate ~~mass~~inventories. With the exception of the Middle Triassic Bravaisberget Formation, all Mesozoic units exhibit MSR-trend~~-based~~ estimates that overlap the long-term trend but rate~~-based~~ estimates that fall below it (Fig. 10). As discussed above, we infer that this pattern reflects anomalously high measured

$\partial\delta^{34}S_{CAS}/\partial t(max)$ values as a consequence of rapid evolution of seawater sulfate $\delta^{34}S$ within semi-restricted -marine basins of the proto-Atlantic and western Tethys oceans. Cambrian units exhibit a wide range of $[SO_4^{2-}]_{SW}$ estimates, although a cluster of results falls just below the long-term trend, with many estimates between 1 and 5 mM (Fig. 10). We infer that either our long-term record (Fig. 4) overestimates $[SO_4^{2-}]_{SW}$ for the Cambrian, or the studied units are biased toward low $[SO_4^{2-}]_{SW}$. Late Neoproterozoic units exhibit an even wider range of $[SO_4^{2-}]_{SW}$ estimates than Cambrian units and lack any apparent clustering (Fig. 10). However, all but one of these units yield similar $[SO_4^{2-}]_{SW}$ estimates for the MSR-trend and rate methods (Fig. 6), suggesting that the estimates are robust. We infer ~~that either~~ that the late Neoproterozoic (635-542 Ma) was characterized by a highly unstable marine sulfur cycle, as a consequence of which seawater sulfate concentrations ~~were highly variable during the Neoproterozoic~~varied tremendously. This inference is supported by some earlier studies (Li et al., 2010; Loyd et al., 2012, 2013), although other studies have ~~, or problems with rate estimation and sample diagenesis have generated considerable noise in our dataset. W~~inferred low (Hurtgen et al., 2002, 2005, 2006; Ries et al., 2009) or monotonically rising sulfate concentrations (Halverson and Hurtgen, 2007) during this interval~~e are inclined toward the interpretation of high seawater sulfate variability during the Neoproterozoic because all but one of the units in Figure 6 yielded similar $[SO_4^{2-}]_{SW}$ estimates for the MSR-trend and rate methods, suggesting that the calculated values are robust. Previous studies of Neoproterozoic seawater sulfate have generally inferred low (Hurtgen et al., 2002, 2005, 2006; Ries et al., 2009) or monotonically rising concentrations (Halverson and Hurtgen, 2007), but our findings imply a highly unstable marine S cycle with possible rapid fluctuations between high and low seawater sulfate concentrations from ~635 to 542 Ma~~.

5 Conclusions

The ~~two~~ rate and MSR-trend methods developed in this study for quantifying paleo-seawater sulfate concentrations ~~in paleo-seawater~~ are complementary and quasi-~~largely~~ independent, providing estimates of maximum and mean $[SO_4^{2-}]_{SW}$, respectively, f~~f~~or ~~the~~ a ~~time interval~~paleomarine unit of interest. Both techniques make use of $\Delta^{34}S_{CAS\text{-}PY}$, i.e., the isotopic fractionation associated with microbial sulfate reduction (MSR). The ~~"~~rate method~~"~~ evaluates $[SO_4^{2-}]_{SW}$ as a function of $\partial\delta^{34}S_{CAS}/\partial t(max)$, i.e., the maximum observed rate of change in seawater sulfate, whereas the ~~"~~MSR-trend method~~"~~ makes use of an empirical relationship between ~~the~~ MSR fractionation ~~associated with MSR~~ and ~~ambient~~ aqueous sulfate concentrations. The significance of our quantitative approach is that estimates of paleo-seawater $[SO_4^{2-}]$ can be derived from two readily measurable sedimentary parameters~~:~~, $\Delta^{34}S_{CAS\text{-}PY}$ and $\delta^{34}S_{CAS}/\partial t(max)$. Based on these methods, ~~A~~an analysis of long-term variation ~~in seawater sulfate concentrations~~ since ~~630~~ 635 Ma ~~based on these methods~~ suggests that $[SO_4^{2-}]_{SW}$ was low during the late Neoproterozoic (<5 mM), rose sharply across the Ediacaran/Cambrian boundary (to ~5-10 mM), and rose again during the Permian to near-modern levels (~10-30 mM). However, high-resolution $\delta^{34}S_{CAS}$ studies provide evidence of ~~repeated~~ episodic ~~short-term~~high-frequency (<~2-Myr) events during which ~~drawdown of~~ seawater sulfate concentrations ~~during the Phanerozoic, i~~were drawn down in response to

massive evaporite deposition, ~~n and/or~~ reduced sediment ventilation and increased pyrite burial in the aftermath of mass extinctions, or other factors. The techniques developed in this study for quantitative analysis of paleo-seawater [SO_4^{2-}] should be applicable to ~~sediments~~ marine units of any age provided that (1) MSR fractionation ~~during MSR~~ has been a conservative process through time (i.e., the dominant pathways of sulfur metabolism have not changed greatly), and (2) ~~reasonable~~ sufficient time control exists for estimation of rates of $\delta^{34}S_{CAS}$ variation. ~~Given a sufficient number of~~ As more S-isotopic studies of cogenetic sulfate and sulfide become available, it should ultimately be possible to reconstruct variation in seawater sulfate concentrations throughout Earth history.

Author Contributions

TJA developed the project concept and modeling methodology, GML, HYS, TWL, and DEC provided isotopic data, and all authors assisted in drafting the manuscript.

Acknowledgments

Research by TJA and TWL is supported by the Sedimentary Geology and Paleobiology program of the U.S. National Science Foundation and the NASA Exobiology program. TJA also gratefully acknowledges support from the State Key Laboratory of Geological Processes and Mineral Resources, China University of Geosciences, Wuhan (program GPMR201301).

Appendix A: Data tables

The primary sulfur isotopic data and model output for this study are given in Tables A1 to A4.

Table A1. MSR fractionation data for modern aqueous systems

Table A2. Phanerozoic $\delta^{34}S_{CAS}$ data

Table A3. Modeled Phanerozoic seawater sulfate $\delta^{34}S$ curve

Table A4. Analysis of high-frequency seawater sulfate variation

Appendix B: Extended discussion

B1 Relationship of rate of seawater sulfate change to sulfate residence time

The maximum possible rate of change in seawater sulfate $\delta^{34}S$ (i.e., $\partial\delta^{34}S_{SO4}/\partial t(max)$) is inversely proportional to the residence time of sulfate in seawater (τ). The exact quantitative form of this relationship can be derived from Equation 2 of Algeo et al. (2014), reorganization of which yields:

$$M_{SW} / F_{PY} = k_1 \times \Delta^{34}S_{CAS\text{-}PY} / \partial\delta^{34}S_{CAS}/\partial t(max) \quad (B1)$$

The residence time of sulfur in seawater is equal to the mass of seawater sulfate divided by the total sink flux, i.e., the reduced sulfur flux (F_{PY}) plus the oxidized sulfur flux (F_{EVAP}):

$$\tau = M_{SW} / (F_{PY} + F_{EVAP}) \quad (B2)$$

Letting ϕ_{PY} be the fraction of the total S flux represented by pyrite burial (i.e., $F_{PY} / (F_{PY} + F_{EVAP})$), then:

$$\tau \times \phi_{PY}^{-1} = M_{SW} / F_{PY} \quad (B3)$$

And substitution into Equation B1 yields:

$$\tau \times \phi_{PY}^{-1} = k_1 \times \Delta^{34}S_{CAS\text{-}PY} / \partial\delta^{34}S_{CAS}/\partial t(max) \quad (B4)$$

This equation quantifies the inverse proportionality between the maximum rate of change of seawater sulfate $\delta^{34}S$ and the residence time of sulfur in seawater.

B2 Effects of $[SO_4^{2-}]_{SW}$-dependent pyrite burial fluxes on $[SO_4^{2-}]_{SW}$ estimates

Although we made use of fixed estimates of the pyrite burial flux (F_{PY}), i.e., 4×10^{13} g yr^{-1} for oxic oceans and 10×10^{13} g yr^{-1} for anoxic oceans, it is possible that F_{PY} is dependent on $[SO_4^{2-}]_{SW}$. Wortmann and Chernyavsky (2007) inferred a non-linear positive relationship of F_{PY} with $[SO_4^{2-}]_{SW}$ (their figure 4). We explored the effects of varying pyrite burial fluxes on seawater sulfate estimates as follows. Equations 2-3 have four variables: $[SO_4^{2-}]_{SW}$ (or M_{SW}, since these are inter-convertible via Equation 4), F_{PY}, $\Delta^{34}S_{CAS\text{-}PY}$, and $\partial\delta^{34}S_{SO4}/\partial t$. However, $\Delta^{34}S_{CAS\text{-}PY}$ can be modeled as a function of $[SO_4^{2-}]_{SW}$ (i.e., the MSR trend of Figure 2 and Equation 6), reducing the number of potentially independent variables to three (we state "potentially independent" as there may in fact be some dependency among these variables). Now it is possible to explore the effects of simultaneous variations in $[SO_4^{2-}]_{SW}$ and F_{PY} on $\partial\delta^{34}S_{SO4}/\partial t(max)$ via a modified form of Equation 2:

$$\partial\delta^{34}S_{CAS}/\partial t(max) = k_1 \times k_2 \times F_{PY} \times \exp(\log[SO_4^{2-}]_{SW} * 0.42 + 1.10) / [SO_4^{2-}]_{SW} \quad (B5)$$

The three modeled parameters exhibit log-linear relationships, with larger $\partial\delta^{34}S_{CAS}/\partial t(max)$ associated with larger $[SO_4^{2-}]_{SW}$ and F_{PY} (Fig. B1). $\partial\delta^{34}S_{CAS}/\partial t(max)$ scales linearly with F_{PY}, so

Formatted ...
Formatted: Font color: Auto
Formatted ...
Formatted: Indent: First line: 0.5"
Formatted ...
Formatted ...

uncertainty in the latter parameter is directly mirrored in the former parameter. The range of F_{PY} used in our study (i.e., 4-10 × 10^{13} g yr^{-1}) is consistent with variation in $\partial\delta^{34}S_{CAS}/\partial t(max)$ from ~1 to 100 ‰ Myr^{-1}. The F_{PY}-$[SO_4^{2-}]_{SW}$ relationship of Wortmann and Chernyavsky (2007, their figure 4; red curve, Fig. B1), if correct, indicates that variation in $\partial\delta^{34}S_{CAS}/\partial t(max)$ cannot exceed ~3 ‰ Myr^{-1} under any set of conditions.

We tested the influence of sulfate-dependent pyrite burial fluxes on seawater sulfate concentration estimates by applying the relationship of Wortmann and Chernyavsky (2007) to our rate-method calculations. Their relationship can be reduced to a logarithmic expression:

$$F_{PY} = 0.7681 \times \ln([SO_4^{2-}]_{SW}) + 1.405 \quad \text{(B6)}$$

where F_{PY} is in units of 10^{13} g yr^{-1} (rather than in mol yr^{-1}, as in their paper) and $[SO_4^{2-}]_{SW}$ is in units of mM. This expression yielded a r^2 of 0.98 in relation to Wortmann and Chernyavsky's curve (their figure 4). In making use of sulfate-dependent pyrite burial fluxes for calculation of seawater sulfate concentration estimates, Equations 3 and 4 must be reorganized as follows:

$$[SO_4^{2-}]_{SW}(max) / F_{PY} = k_1 \times k_2 \times \Delta^{34}S_{CAS\text{-}PY} / \partial\delta^{34}S_{CAS}/\partial t(max) \quad \text{(B7)}$$

Although Equation B7 has two unknowns, i.e., $[SO_4^{2-}]_{SW}(max)$ and F_{PY}, it can be solved because F_{PY} is a function of $[SO_4^{2-}]_{SW}$ in figure 4 of Wortmann and Chernyavsky (2007). The empirical relationship between $[SO_4^{2-}]_{SW}$ and $[SO_4^{2-}]_{SW}(max) / F_{PY}$ is given by the polynomial equation:

$$[SO_4^{2-}]_{SW}(max) / F_{PY} = -0.0018([SO_4^{2-}]_{SW})^2 + 0.2842([SO_4^{2-}]_{SW}) + 0.4651 \quad \text{(B8)}$$

With substitution and reorganization, Equations B7 and B8 yield:

$$0 = -0.0018([SO_4^{2-}]_{SW})^2 + 0.2842([SO_4^{2-}]_{SW}) + (0.4651 - k_1 \times k_2 \times \Delta^{34}S_{CAS\text{-}PY}/[\partial\delta^{34}S_{CAS}/\partial t(max)]) \quad \text{(B9)}$$

This second-order polynomial equation can now be solved for $[SO_4^{2-}]_{SW}$ using the quadratic solution, after which F_{PY} can be calculated from Equation B6.

Using Equation B9, we calculated $[SO_4^{2-}]_{SW}$ on the basis of $\partial\delta^{34}S_{CAS}/\partial t(max)$ and $\Delta^{34}S_{CAS\text{-}PY}$. These relationships are plotted as variation in $\partial\delta^{34}S_{CAS}/\partial t(max)$ as a function of $[SO_4^{2-}]_{SW}$ and $\Delta^{34}S_{CAS\text{-}PY}$ (Fig. B2; cf. Figure 1). At high $[SO_4^{2-}]_{SW}$, the two sets of $\partial\delta^{34}S_{CAS}/\partial t(max)$ curves are nearly co-linear, which is because the value of F_{PY} in figure 4 of Wortmann and Chernyavsky (2007) for $[SO_4^{2-}]_{SW}$ >10 mM is nearly invariant and similar to the flux that we used for oxic marine environments (i.e., 4 × 10^{13} g yr^{-1}). In contrast, the two sets of curves diverge sharply at

Formatted ...
Formatted: Indent: First line: 0.5"
Formatted ...
Formatted ...
Formatted ...
Formatted ...
Formatted ...
Formatted ...
Formatted ...
Formatted ...
Formatted ...
Formatted ...

$[SO_4^{2-}]_{SW}$ <1 mM, which is a consequence of the much lower F_{PY} values associated with low seawater sulfate concentrations in the Wortmann and Chernyavsky curve.

The $\partial\delta^{34}S_{CAS}/\partial t(max)$ curves based on the sulfate-dependent pyrite fluxes of Wortmann and Chernyavsky (2007) require comment. First, the MSR trend (Figure 2) corresponds almost entirely to a limited range of $\partial\delta^{34}S_{CAS}/\partial t(max)$ values (i.e., 2 to 4; Fig. B2). This suggests that there ought to be quite limited variation in $\partial\delta^{34}S_{CAS}/\partial t(max)$ over a wide range of seawater sulfate concentrations in nature. Second, many combinations of the two sediment parameters that can be measured (i.e., $\Delta^{34}S_{CAS\text{-}PY}$ and $\partial\delta^{34}S_{CAS}/\partial t(max)$) cannot yield a $[SO_4^{2-}]_{SW}$ estimate. For example, no $[SO_4^{2-}]_{SW}$ estimate is possible for $\Delta^{34}S_{CAS\text{-}PY}$ of 7‰ in combination with any $\partial\delta^{34}S_{CAS}/\partial t(max)$ value that is larger than ~4 (Fig. B2). This situation exists because high rates of variation in seawater sulfate $\delta^{34}S$ are not possible where the pyrite burial flux is sharply curtailed by $[SO_4^{2-}]_{SW}$-dependency (as in figure 4 of Wortmann and Chernyavsky, 2007). However, many paleomarine units exhibit $\partial\delta^{34}S_{CAS}/\partial t(max)$ values outside the narrow range permitted by the Wortmann and Chernyavsky (2007) relationship (see Table A4 and Figures 6-8). If the Wortmann and Chernyavsky (2007) parameterization of the F_{PY}-$[SO_4^{2-}]_{SW}$ relationship is correct, then one must conclude either that all of these published higher rates are products of uncertain geochronologic dating, diagenetic artifacts, or sample processing and analytical problems. On the other hand, the use of fixed values for F_{PY} in our rate-method calculations (Eqs. 2-4) yields estimates of $[SO_4^{2-}]_{SW}$ that are—for the most part—consistent with estimates of $[SO_4^{2-}]_{SW}$ based on the MSR-trend method (Section 2.2; see Figures 6-8 for examples). We acknowledge that some form of sulfate-dependency of pyrite burial fluxes may exist but suggest that it may differ from the relationship given by Wortmann and Chernyavsky (2007).

B3 Sources of sulfide $\delta^{34}S$ data

Although all sulfate $\delta^{34}S$ data used in the calculation of $\Delta^{34}S_{sulfate\text{-}sulfide}$ values in Figure 2 are based on aqueous SO_4^{2-} measurements, we used sulfide $\delta^{34}S$ data from multiple sources: pyrite, sediment acid-volatile sulfur (AVS), sediment total reduced sulfur (TRS), and aqueous H_2S (Table A1). We have constructed a version of Figure 2 that shows the different sulfide phases, and we calculated separate regressions for each phase (Fig. B3). The following points should be noted about this figure. First, each of the four phases yields a statistically significant regression (r = 0.81-0.92; $p(\alpha)$ <0.05; Table B1). Second, the four phases have similar regression slopes although slightly variable y-intercepts. For this reason, TRS and AVS yield $\Delta^{34}S_{CAS\text{-}PY}$ values that are, on average, slightly larger for a given $[SO_4^{2-}]_{SW}$ than pyrite and aqueous H_2S. Third, the four regression lines generally converge at higher $[SO_4^{2-}]_{SW}$, and the largest differences occur at low $[SO_4^{2-}]_{SW}$, where data is sparser.

One point that bears reflection is that estimates of paleoseawater $[SO_4^{2-}]_{SW}$ are based not on aqueous sulfide $\delta^{34}S$, which cannot be measured for paleomarine systems, but on mineral sulfide (generally pyrite) $\delta^{34}S$. Therefore, the critical relationship for establishing a viable MSR-trend proxy for $[SO_4^{2-}]_{SW}$ is that between sulfate $\delta^{34}S$ and pyrite $\delta^{34}S$. Although we could have used the pyrite $\delta^{34}S$ data alone, we opted to include other sulfide phases to produce a larger sulfide $\delta^{34}S$ dataset, especially one containing more data at low $[SO_4^{2-}]_{SW}$, with the goal

Formatted ...

Formatted ...

Formatted: Adjust space between Latin and Asian text, Adjust space between Asian text and numbers

Formatted ...

Formatted: Font color: Auto

Formatted: Indent: First line: 0.5"

Formatted ...

Formatted: Indent: First line: 0.5", Space After: 0 pt, Don't adjust space between Latin and Asian text, Don't adjust space between Asian text and numbers

Formatted ...

of generating a stable relationship over a wider range of $[SO_4^{2-}]_{SW}$ values. Whether there are real differences in the regression relationships among these four sulfide phases is an issue that will require further inquiry. These sulfide phases yield similar relationships between $\Delta^{34}S_{sulfate\text{-}sulfide}$ and $[SO_4^{2-}]_{SW}$ that, based on the available data, are statistically indistinguishable (Fig. B3).

Table B1. Regression statistics for reduced sulfur phases (see Figure B3)

Sulfur phase	*n*	*r*	*m*	*b*	*p(α)*
Pyrite	48	0.92	0.46	-0.35	<0.01
Sediment AVS	6	0.81	0.42	-0.06	<0.05
Sediment TRS	11	0.89	0.33	0.20	<0.01
Aqueous H_2S	16	0.84	0.44	-0.20	<0.01

Figure B1. Relationship of $\partial\delta^{34}S_{CAS}/\partial t(max)$ to F_{PY} and $[SO_4^{2-}]_{SW}$, with $\Delta^{34}S_{CAS\text{-}PY}$ estimated as a function of $[SO_4^{2-}]_{SW}$ (Figure 2, Equation 6). The dashed horizontal lines represent the pyrite burial fluxes used in this study for oxic and anoxic paleomarine systems, i.e., 4×10^{13} g yr^{-1} and 10×10^{13} g yr^{-1}, respectively. The red line represents the $[SO_4^{2-}]_{SW}$-dependency of the pyrite burial flux as given by Wortmann and Chernyavsky (2007, their figure 4). Note that according to the latter relationship, $\partial\delta^{34}S_{CAS}/\partial t(max)$ values cannot exceed ~3 ‰ Myr^{-1} under any set of conditions.

Figure B2. $\partial\delta^{34}S_{CAS}/\partial t(max)$ values calculated using fixed pyrite burial fluxes (blue diagonal lines; cf. Figure 1) and the sulfate-dependent pyrite burial fluxes of Wortmann and Chernyavsky (2007; red curves). Note that, for the latter curves, many combinations of the two measured sediment parameters ($\Delta^{34}S_{CAS\text{-}PY}$ and $\partial\delta^{34}S_{CAS}/\partial t(max)$) cannot yield a $[SO_4^{2-}]_{SW}$ estimate. Shown for reference is the MSR trend of Figure 2.

Figure B3. Replotted MSR trend data (from Figure 2, Table A1) as a function of sulfide $\delta^{34}S$ source (symbols as given in legend). Separate regressions for the four different sulfide phases (dashed lines) show small differences in slopes and y-intercepts (Table B1), although the regression lines are statistically indistinguishable.

Formatted ...

Formatted: Font: 12 pt

Formatted: Space After: 0 pt, Don't adjust space between Latin and Asian text, Don't adjust space between Asian text and numbers

Formatted ...

Formatted ...

Formatted ...

References

Adams, D. D., Hurtgen, M. T. and Sageman, B. B.: Volcanic triggering of a biogeochemical cascade during Oceanic Anoxic Event 2. Nat. Geosci., 3, 201-204, 2010.

Algeo, T. J., Meyers, P. A., Robinson, R. S., Rowe, H. and Jiang, G. Q.: Icehouse-greenhouse variations in marine denitrification. Biogeosciences, 11, 1273-1295, 2014.

Asmussen, G. and Strauch, G.: Sulfate reduction in a lake and the groundwater of a former lignite mining area studied by stable sulfur and carbon isotopes. Water Air Soil Poll., 108, 271-284, 1998.

Bates, A. L., Spiker, E. C., Hatcher, P. G., Stout, S. A. and Weintraub, V. C.: Sulfur geochemistry of organic-rich sediments from Mud Lake, Florida, U.S.A. Chem. Geol., 121, 245-262, 1995.

Bates, A. L., Spiker, E. C. and Holmes, C. W.: Speciation and isotopic composition of sedimentary sulfur in the Everglades, Florida, USA. Chem. Geol., 146, 155-170, 1998.

Bates, A. L., Spiker, E. C., Orem, W. H. and Burnett, W.C.: Speciation and isotopic composition of sulfur in sediments from Jellyfish Lake, Palau. Chem. Geol., 106, 63-76, 1993.

Bekker, A., Holland, H. D., Wang, P. L., Rumble, D., III, Stein, H. J., Hannah, J. L., Coetzee, L. L. and Beukes, N. J.: Dating the rise of atmospheric oxygen. Nature, 427, 117-120, 2004.

Bergman, N. M., Lenton, T. M. and Watson, A. J.: COPSE: a new model of biogeochemical cycling over Phanerozoic time. Am. J. Sci., 397-437, 2004.

Berner, R. A.: A model for calcium, magnesium and sulfate in seawater over Phanerozoic time. Am. J. Sci., 304, 438-453, 2004.

Berner, Z. A., Puchelt, H., Nöltner, T. and Kramar, U.: Pyrite geochemistry in the Toarcian Posidonia Shale of southwest Germany: evidence for contrasting trace-element patterns of diagenetic and syngenetic pyrites. Sedimentology, 60, 548-573, 2013.

Berra, F., Jadoul, F. and Anelli, A.: Environmental control on the end of the Dolomia Principale/Hauptdolomit depositional system in the central Alps: coupling sea-level and climate changes. Palaeogeogr. Palaeoclimatol. Palaeoecol., 290, 138-150, 2010.

Böttcher, M. E., Voss, M., Schulz-Bull, D., Schneider, R., Leipe, T. and Knöller, K.: Environmental changes in the Pearl River Estuary (China) as reflected by light stable isotopes and organic contaminants. J. Mar. Syst., 82, S43-S53, 2010.

Bottrell, S. H. and Newton, R. J.: Reconstruction of changes in global sulfur cycling from marine sulfate isotopes. Earth-Sci. Rev., 75, 59-83, 2006.

Bradley, A. S., Leavitt, W. D. and Johnston, D. T.: Revisiting the dissimilatory sulfate reduction pathway. Geobiology, 9, 446-457, 2011.

Brennan, S. T., Lowenstein, T. K. and Horita, J.: Seawater chemistry and the advent of biocalcification. Geology, 32, 473-476, 2004.

Brüchert, V.: Physiological and ecological aspects of sulfur isotope fractionation during bacterial sulfate reduction, in: Amend, J. P., Edwards, K. J. and Lyons, T. W. (Eds.), Sulfur Biogeochemistry—Past and Present, Geol. Soc. Am. Spec. Pap., 379, 1-16, 2004.

Brüchert, V. and Pratt, L. M.: Contemporaneous early diagenetic formation of organic and inorganic sulfur in estuarine sediments from St. Andrew Bay, Florida, USA. Geochim. Cosmochim. Acta, 60, 2325-2332, 1996.

Formatted: Font: (Default) Calibri, 12 pt, Not Bold, Do not check spelling or grammar

Formatted: Font: (Default) Calibri, 12 pt, Do not check spelling or grammar

Formatted: Font: (Default) Calibri, 12 pt, Do not check spelling or grammar

Brüchert, V. and Pratt, L. M.: Stable sulfur isotopic evidence fro historical changes of sulfur cycling in estuarine sediments from northern Florida. Aquat. Geochem., 5, 249-268, 1999.

Brüchert, V., Knoblauch, C. and Jørgensen, B. B.: Microbial controls on the stable sulfur isotope fractionation during bacterial sulfate reduction in Arctic sediments. Geochim. Cosmochim. Acta, 65, 753-766, 2001.

Brunner, B. and Bernasconi, S. M.: A revised isotope fractionation model for dissimilatory sulfate reduction in sulfate-reducing bacteria. Geochim. Cosmochim. Acta, 69, 4759-4771, 2005.

Canfield, D. E.: A new model for Proterozoic ocean chemistry. Nature, 396, 450-453, 1998.

Canfield, D. E.: Isotope fractionation by natural populations of sulfate-reducing bacteria. Geochim. Cosmochim. Acta, 65, 1117-1124, 2001.

Canfield, D. E.: The evolution of the Earth surface sulfur reservoir. Am. J. Sci., 304, 839-861, 2004.

Canfield, D. E. and Farquhar, J.: Animal evolution, bioturbation, and the sulfate concentration of the oceans. Proc. Nat. Acad. Sci. (U.S.A.), 106, 8123-8127, 2009.

Canfield, D. E. and Raiswell, R.: The evolution of the sulfur cycle. Am. J. Sci., 299, 697-723, 1999.

Canfield, D. E. and Thamdrup, B. T.: The production of ^{34}S-depleted sulfide during disproportionation of elemental sulfur. Science, 266, 1973-1975, 1994.

Canfield, D. E., Raiswell, R. and Bottrell, S.: The reactivity of sedimentary iron minerals toward sulfide. Am. J. Sci., 292, 659-683, 1992.

Canfield, D. E., Olesen, C. A. and Cox, R. P.: Temperature and its control of isotope fractionation by a sulfate-reducing bacterium. Geochim. Cosmochim. Acta, 70, 548-561, 2006.

Canfield, D. E., Poulton, S. W. and Narbonne, G. M.: Late-Neoproterozoic deep-ocean oxygenation and the rise of animal life. Science, 315, 92-95, 2007.

Canfield, D. E., Farquhar, J. and Zerkle, A. L.: High isotope fractionations during sulfate reduction in a low-sulfate euxinic ocean analog. Geology, 38, 415-418, 2010.

Chambers, L. A., Trudinger, P. A., Smith, J. W. and Burns, M. S.: Fractionation of sulfur isotopes by continuous cultures of *Desulfovibrio desulfuricans*. Can. J. Microbiol., 21, 1602-1607, 1975.

Chanton, J. P. and Lewis, F. G.: Plankton and dissolved inorganic carbon isotopic composition in a river-dominated estuary: Apalachicola Bay, Florida. Estuaries, 22, 575-583, 1999.

Detmers, J., Brüchert, V., Habicht, K. S. and Kuever, J.: Diversity of sulfur isotope fractionations by sulfate-reducing prokaryotes. Appl. Environ. Microbiol., 67, 888-894, 2001.

DiMichele, W. A. and Hook, R. W.: Paleozoic terrestrial ecosystems, in: Behrensmeyer, A. K., et al. (Eds.), Terrestrial Ecosystems through Time, The University of Chicago Press, 205-325, 1992.

Doi, H., Kikuchi, E., Mizota, C., Satoh, N., Shikano, S., Yurlova, N., Yadrenkina, E. and Zuykova, E.: Carbon, nitrogen, and sulfur isotope changes and hydro-geological processes in a saline lake chain. Hydrobiologia, 529, 225-235, 2004.

Eckert, T., Brunner, B., Edwards, E. A. and Wortmann, U.G.: Microbially mediated re-oxidation of sulfide during dissimilatory sulfate reduction by *Desulfobacter latus*. Geochim. Cosmochim. Acta, 75(12), 3469-3485, 2011.

Formatted: Indent: Left: 0", Hanging: 0.5", Space Before: 0 pt, After: 0 pt, Adjust space between Latin and Asian text, Adjust space between Asian text and numbers

966 Farquhar, J., Peters, M., Johnston, D. T., Strauss, H., Masterson, A., Wiechert, U. and Kaufman,
967 A. J.: Isotopic evidence for Mesoarchaean anoxia and changing atmospheric sulphur
968 chemistry. Nature, 449, 706-710, 2007.
969 Fike, D. A. and Grotzinger, J. P.: A paired sulfate-pyrite $\delta^{34}S$ approach to understanding the
970 evolution of the Ediacaran-Cambrian sulfur cycle. Geochim. Cosmochim. Acta, 72, 2636-
971 2648, 2008.
972 Fike, D. A., Grotzinger, J. P., Pratt, L. M. and Summons, R. E.: Oxidation of the Ediacaran Ocean.
973 Nature, 444, 744-747, 2006.
974 Fry, B.: Sources of carbon and sulfur nutrition for consumers in three meromictic lakes of New
975 York State. Limnol. Oceanogr., 31, 79-88, 1986a.
976 Fry, B.: Stable sulfur isotopic distributions and sulfate reduction in lake sediments of the
977 Adirondacks Mountains, New York. Biogeochemistry, 2, 329-343, 1986b.
978 Fry, B., Giblin, A. and Dornblaser, M.: Stable sulfur isotopic compositions of chromium-reducible
979 sulfur in lake sediments, in: Vairavamurthy, A. and Schoonens, M. A. A. (Eds.),
980 Geochemical Transformation of Sedimentary Sulfur, American Chemical Society, ACS
981 Symposium Series, 612, 397-410, 1995.
982 Fry, B., Jannasch, H. W., Molyneaux, S. J., Wirsen, C. O., Muramoto, J. A. and King, S.: Stable
983 isotope studies of the carbon, nitrogen and sulfur cycles in the Black Sea and the Cariaco
984 Trench. Deep-Sea Res., A38(Suppl. 2), S1003-S1019, 1991.
985 Gellatly, A. M. and Lyons, T. W.: Trace sulfate in mid-Proterozoic carbonates and the sulfur
986 isotope record of biospheric evolution. Geochim. Cosmochim. Acta, 69, 3813-3829,
987 2005.
988 Gill, B. C., Lyons, T. W. and Saltzman, M. R.: Parallel, high-resolution carbon and sulfur isotope
989 records of the evolving Paleozoic marine sulfur reservoir. Palaeogeogr. Palaeoclimatol.
990 Palaeoecol., 256, 156-173, 2007.
991 Gill, B. C., Lyons, T. W., Young, S. A., Kump, L. R., Knoll, A. H. and Saltzman, M. R.: Geochemical
992 evidence for widespread euxinia in the Later Cambrian ocean. Nature, 469, 80-83,
993 2011a.
994 Gill, B. C., Lyons, T. W. and Jenkyns, H. C.: A global perturbation to the sulfur cycle during the
995 Toarcian Oceanic Anoxic Event. Earth Planet. Sci. Lett., 312, 484-496, 2011b.
996 Gomes, M. L. and Hurtgen, M. T.: Sulfur isotope systematics of a euxinic, low-sulfate lake:
997 evaluating the importance of the reservoir effect in modern and ancient oceans.
998 Geology, 41, 663-666, 2013.
999 Gorlenko, V. M. and Chebotarev, E. N.: Microbiologic processes in meromictic Lake Sakovo.
1000 Microbiology, 50, 134-139, 1981.
1001 Gorlenko, V. M., Vainstein, B. and Kachalkin, V. I.: Microbiological characteristic of Lake
1002 Mogilnoe. Arch. Hydrobiol., 81, 475-492, 1978.
1003 Gradstein, F. M., Ogg, J. G., Schmitz, M. D. and Ogg, G. M.: The Geologic Time Scale 2012.
1004 Elsevier, Amsterdam, 2 vol., 2012.
1005 Habicht, K. S. and Canfield, D. E.: Sulphur isotope fractionation in modern microbial mats and
1006 the evolution of the sulphur cycle. Nature, 382, 342-343, 1996.
1007 Habicht, K. S. and Canfield, D. E.: Sulfur isotope fractionation during bacterial sulfate reduction
1008 in organic-rich sediments. Geochim. Cosmochim. Acta, 61, 5351-5361, 1997.

Habicht, K. S. and Canfield, D. E.: Isotope fractionation by sulfate-reducing natural populations and the isotopic composition of sulfide in marine sediments. Geology, 29, 555-558, 2001.

Habicht, K. S., Gade, M., Thamdrup, B., Berg, P. and Canfield, D. E.: Calibration of sulfate levels in the Archean ocean. Science, 298, 2372-2374, 2002.

Halevy, I., Peters, S. E. and Fischer, W. W.: Sulfate burial constraints on the Phanerozoic sulfur cycle. Science, 337, 331-334, 2012.

Halverson, G. P. and Hurtgen, M. T.: Ediacaran growth of the marine sulfate reservoir. Earth Planet. Sci. Lett., 263, 32-44, 2007.

Halverson, G. P., Hoffman, P. F., Schrag, D. P., Maloof, A. C. and Rice, A. H. N.: Toward a Neoproterozoic composite carbon-isotope record. Geol. Soc. Am. Bull., 117, 1181-1207, 2005.

Hartmann, M. and Nielsen, H.: δ^{34}S-Werte in rezenten Meeressedimenten und ihre Deutung am Beispiel einiger Sedimentprofile aus der westlichen Ostsee. Geol. Rundsch., 58, 621-655, 1968.

Holland, H. D.: Volcanic gases, black smokers, and the Great Oxidation Event. Geochim. Cosmochim. Acta, 66, 3811-3826, 2002.

Holser, W., Maynard, J. B. and Cruikshank, K.: Modelling the natural cycle of sulphur through Phanerozoic time, in: Brimblecombe, P. and Lein, A. Y. (Eds.), Evolution of the Global Biogeochemical Sulfur Cycle, Wiley, New York, 21-56, 1989.

Horita, J., Zimmermann, H. and Holland, H. D.: Chemical evolution of seawater during the Phanerozoic: Implications from the record of marine evaporites. Geochim. Cosmochim. Acta, 66, 3733-3756, 2002.

Hurtgen, M. T., Arthur, M. A., Suits, N. S. and Kaufman, A. J.: The sulfur isotopic composition of Neoproterozoic seawater sulfate: implications for a snowball Earth? Earth Planet. Sci. Lett., 203, 413-429, 2002.

Hurtgen, M. T., Arthur, M. A. and Halverson, G. P.: Neoproterozoic sulfur isotopes, the evolution of microbial sulfur species, and the burial efficiency of sulfide as sedimentary pyrite. Geology, 33, 41-44, 2005.

Hurtgen, M. T., Halverson, G. P., Arthur, M. A. and Hoffman, P. F.: Sulfur cycling in the aftermath of a 635-Ma snowball glaciation: Evidence for a syn-glacial sulfidic deep ocean. Earth Planet. Sci. Lett., 245, 551-570, 2006.

Ivanov, M. V., Rusanov, I. I., Pimenov, N. V., Bairamov, I. T., Yusupov, S. K., Savvichev, A. S., Lein, A. Y. and Sapozhnikov, V. V.: Microbial processes of the carbon and sulfur cycles in Lake Mogil'noe. Microbiology, 70, 583-593, 2001.

Johnston, D. T.: Multiple sulfur isotopes and the evolution of Earth's surface sulfur cycle. Earth-Sci. Rev., 106, 161-183, 2011.

Johnston, D. T., Wing, B. A., Farquhar, J., Kaufman, A. J., Strauss, H., Lyons, T. W., Kah, L. C. and Canfield, D. E.: Active microbial sulfur disproportionation in the Mesoproterozoic. Science, 310, 1477-1479, 2005.

Johnston, D. T., Farquhar, J., Habicht, K. S. and Canfield, D. E.: Sulphur isotopes and the search for life: strategies for identifying sulphur metabolisms in the rock record and beyond. Geobiology, 6, 425-435, 2008.

Jones, B. A., Facchetti, A., Wasielewski, M. R. and Marks, T. J.: Theory of oxidation-reduction reactions involving electron transfer. 5. Comparison and properties of electrochemical and chemical rate constants. J. Am. Chem. Soc., 129, 15259-15278, 2007.
Jørgensen, B. B.: Mineralization of organic matter in the sea bed—the role of sulphate reduction. Nature, 296, 643-645, 1982.
Jørgensen, B. B. and Cohen, Y.: Solar Lake (Sinai). 5. The sulfur cycle of the benthic cyanobacterial mats. Limnol. Oceanogr., 22, 657-666, 1977.
Kah, L. C., Lyons, T. W. and Frank, T. D.: Low marine sulphate and protracted oxygenation of the Proterozoic biosphere. Nature, 431, 834-838, 2004.
Kampschulte, A. and Strauss, H.: The sulfur isotopic evolution of Phanerozoic seawater based on the analysis of structurally substituted sulfate in carbonates. Chem. Geol., 204, 255-286, 2004.
Kamyshny, A., Jr., Zerkle, A. L., Mansaray, Z. F., Ciglenečki, I., Bura-Nakić, E., Farquhar, J. and Ferdelman, T. G.: Biogeochemical sulfur cycling in the water column of a shallow stratified sea-water lake: speciation and quadruple sulfur isotope composition. Mar. Geol., 127, 144-154, 2011.
Kaplan, I. R.: Stable isotopes of sulfur, nitrogen and deuterium in Recent marine environments, in: Arthur, M. A., et al. (Eds.), Stable Isotopes in Sedimentary Geology, Society for Sedimentary Geology, Tulsa, Oklahoma, 21-108, 1983.
Kapan, I. R. and Rittenberg, S. C.: Microbiological fractionation of sulphur isotopes. J. Gen. Microbiol., 34, 195-212, 1964.
Kaplan, I. R., Emery, K. O. and Rittenberg, S. C.: The distribution and isotopic abundance of sulphur in recent marine sediments off southern California. Geochim. Cosmochim. Acta, 27, 297-331, 1963.
Karcz, P.: Relationships between development of organic-rich shallow shelf facies and variation in isotopic composition of pyrite (Middle Triassic, Spitsbergen). Polish Polar Research, 31, 239-254, 2010.
Karube, Z., Okada, N. and Tayasu, I.: Sulfur stable isotope signature identifies the source of reduced sulfur in benthic communities in macrophyte zones of Lake Biwa, Japan. Limnology, 13, 269-280, 2012.
Kemp, A. L. W. and Thode, H. G.: The mechanism of the bacterial reduction of sulphate and sulphite from isotope fractionation studies. Geochim. Cosmochim. Acta, 32, 71-91, 1968.
Kleikemper, J., Schroth, M. H., Bernasconi, S. M., Brunner, B. and Zeyer, J.: Sulfur isotope fractionation during growth of sulfate-reducing bacteria on various carbon sources. Geochim. Cosmochim. Acta, 68, 4891-4904, 2004.
Ku, T. C. W., Walter, L. M., Coleman, M. L., Blake, R. E. and Martini, A. M.: Coupling between sulfur recycling and syndepositional carbonate dissolution: evidence from oxygen and sulfur isotope composition of pore water sulfate, South Florida Platform, U.S.A. Geochim. Cosmochim. Acta, 63, 2529-2546, 1999.
Kump, L. R. and Arthur, M. A.: Interpreting carbon-isotope excursions: carbonates and organic matter. Chem. Geol., 161, 181-198, 1999.
Kurtz, A. C., Kump, L. R., Arthur, M. A., Zachos, J. C. and Paytan, A.: Early Cenozoic decoupling of the global carbon and sulfur cycles. Paleoceanography, 18, PA000908, 2003.

Leavitt, W. D., Halevy, I., Bradley, A. S. and Johnston, D. T.: Influence of sulfate reduction rates on the Phanerozoic sulfur isotope record. Proc. Nat. Acad. Sci. (U.S.A.) , 110(28), 11244-11249, 2013.

Lee, Y. J. and Lwiza, K.: Interannual variability of temperature and salinity in shallow water: Long Island Sound, New York. J. Geophys. Res., 110, C09022, 2005.

Lein, A. Y.: Biogeochemistry of the anaerobic diagenesis of Recent Baltic Sea sediments. Environ. Biogeochem., 35, 441-461, 1983.

Li, C., Love, G. D., Lyons, T. W., Fike, D. A., Sessions, A. L. and Chu, X.: A stratified redox model for the Ediacaran ocean. Science, 328, 80-83, 2010.

Li, X., Gilhooly, W. P., III, Zerkle, A. L., Lyons, T. W., Farquhar, J., Werne, J. P., Varela, R. and Scranton, M. I.: Stable sulfur isotopes in the water column of the Cariaco Basin. Geochim. Cosmochim. Acta, 74, 6764-6778, 2010.

Llobet-Brossa, E., Rabus, R., Böttcher, M. E., Könneke, M., Finke, N., Schramm, A., Meyer, R. L., Grötzschel, S., Rosselló-Mora, R. and Amann, R.: Community structure and activity of sulfate-reducing bacteria in an intertidal surface sediment: a multi-method approach. Aquat. Microbial Ecol., 29, 211-226, 2002.

Lojen, S., Ogrinc, N., Dolenec, T., Vokal, B., Szaran, J., Mihelčić, G. and Branica, M.: Nutrient fluxes and sulfur cycling in the organic-rich sediment of Makirina Bay (Central Dalmatia, Croatia). Sci. Total Environ., 327, 265-284, 2004.

Lowenstein, T. K., Hardie, L. A., Timofeeff, M. N. and Demicco, R. V.: Secular variation in seawater chemistry and the origin of calcium chloride basinal brines. Geology, 31, 857-860, 2003.

Lowenstein, T. K., Timofeeff, M. N., Kovalevych, V. M. and Horita, J.: The major-ion composition of Permian seawater. Geochim. Cosmochim. Acta, 69, 1701-1719, 2005.

Loyd, S. J., Marenco, P. J., Hagadorn, J. W., Lyons, T. W., Kaufman, A. J., Sour-Tovar, F. and Corsetti, F. A.: Sustained low marine sulfate concentrations from the Neoproterozoic to the Cambrian: insights from carbonates of northwestern Mexico and eastern California. Earth Planet. Sci. Lett., 339-340, 79-94, 2012.

Loyd, S. J., Marenco, P. J., Hagadorn, J. W., Lyons, T. W., Kaufman, A. J., Sour-Tovar, F. and Corsetti, F. A.: Local $\delta^{34}S$ variability in ~580 Ma carbonates of northwestern Mexico and the Neoproterozoic marine sulfate reservoir. Precambr. Res., 224, 551-569, 2013.

Luo, G. M., Kump, L. R., Wang, Y., Tong, J., Arthur, M. A., Yang, H., Huang, J., Yin, H. and Xie, S.: Isotopic evidence for an anomalously low oceanic sulphate concentration following end-Permian mass extinction. Earth Planet. Sci. Lett., 300, 101-111, 2010.

Luo, G. M., Ono, S., Algeo, T. J., Huang, J., Li, C., Zhou, L., Liu, J, and Xie, S.C.: ~~Ono, S., Huang, J., Li, C., Algeo, T. J., Zhou, L. and Xie, S.:~~ Return of Archean low oceanic sulfate levels during the earliest Mesoproterozoic. ~~Geology, in review~~Precambr. Res., 258, 36-47, 2015.~~.~~

Lyons, T. W.: Sulfur isotopic trends and pathways of iron sulfide formation in upper Holocene sediments of the anoxic Black Sea. Geochim. Cosmochim. Acta, 61, 3367-3382, 1997.

Lyons, T. W. and Gill, B. C.: Ancient sulfur cycling and oxygenation of the early biosphere. Elements 6, 93-99, 2010.

Formatted: Font: 12 pt, Do not check spelling or grammar

Formatted: Font: 12 pt, Do not check spelling or grammar

Formatted: Font: 12 pt, Do not check spelling or grammar

Formatted: Indent: Left: 0", Hanging: 0.5", Space Before: 0 pt, After: 0 pt, Adjust space between Latin and Asian text, Adjust space between Asian text and numbers

Lyons, T. W. and Severmann, S.: A critical look at iron paleoredox proxies: New insights from modern euxinic marine basins. Geochim. Cosmochim. Acta, 70, 5698-5722, 2006.
Mandernack, K. W., Krouse, H. R. and Skei, J. M.: A stable sulfur and oxygen isotopic investigation of sulfur cycling in an anoxic marine basin, Framvaren Fjord, Norway. Chem. Geol., 195, 181-200, 2003.
Mandernack, K. W., Lynch, L., Krouse, H. R. and Morgan, M. D.: Sulfur cycling in wetland peat of the New Jersey Pinelands and its effect on stream water chemistry. Geochim. Cosmochim. Acta, 64, 3949-3964, 2000.
Matrosov, A. G., Chebotarev, N. Ye, Kudryavtseva, A. J., Zyakun, A. M. and Ivanov, M. V.: Sulfur isotopic composition in freshwater lakes containing H_2S. Geokhimiya, 6, 943-7, 1975, and Geochem. Internat., 12, 217-21, 1975.
Mayer, B. and Schwark, L.: A 15,000-year stable isotope record from sediments of Lake Steisslingen, southwest Germany. Chem. Geol., 161, 315-337, 1999.
McArthur, J. M., Donovan, D. T., Thirlwall, M. F., Fouke, B. W. and Mattey, D.: Strontium isotope profile of the early Toarcian (Jurassic) oceanic anoxic event, the duration of ammonite biozones, and belmenite palaeotemperatures. Earth Planet. Sci. Lett., 179, 269-285, 2000.
McFadden, K. A., Huang, J., Chu, X., Jiang, G., Kaufman, A. J., Zhou, C., Yuan, X. and Xiao, S.: Pulsed oxidation and biological evolution in the Ediacaran Doushantuo Formation. Proc. Nat. Acad. Sci. (U.S.A.), 105, 3197-3202, 2008.
Millero, F. J.: Chemical Oceanography, 3rd ed., CRC Press, Boca Raton, Florida, 2005.
Montañez, I.P., et al.: Understanding Earth's Deep Past: Lessons for Our Climate Future, National Academy of Sciences Press, Washington, D.C., 2011.
Nakagawa, M., Ueno, Y., Hattori, S., Umemura, M., Yagi, A., Takai, K., Koba, K., Sasaki, Y., Makabe, A. and Yoshida, N.: Seasonal change in microbial sulfur cycling in monomictic Lake Fukami-ike, Japan. Limnol. Oceanogr., 57, 974-988, 2012.
Nakai, N. and Jensen, M. L.: The kinetic isotope effect in the bacterial reduction and oxidation of sulfur. Geochim. Cosmochim. Acta, 28, 1893-1912, 1964.
Nakai, N., Wada, H., Kiyosu, Y. and Takimoto, M.: Stable isotope studies on the origin and geological history of water and salts in the Lake Vanda area, Antarctica. Geochem. Jour., 9, 7-24, 1975.
Nakano, T., Tayasu, I., Yamada, Y., Hosono, T., Igeta, A., Hyodo, F., Ando, A., Saitoh, Y., Tanaka, T., Wada, E. and Yachi, S.: Effect of agriculture on water quality of Lake Biwa tributaries, Japan. Sci. Total Environ., 389, 132-148, 2008.
Newton, R. J., Reeves, E. P., Kafousia, N., Wignall, P. B., Bottrell, S. H. and Sha, J.-G.: Low marine sulfate concentrations and the isolation of the European epicontinental sea during the Early Jurassic. Geology, 39, 7-10, 2011.
Nriagu, J. O. and Coker, R. D.: Emission of sulfur from Lake Ontario sediments. Limnol. Oceanogr., 21, 485-489, 1976.
Nriagu, J. O. and Harvey, H. H.: Isotopic variation as an index of sulfur poiiution in lakes around Sudbury, Ontario. Nature, 273, 223-224, 1978.
Nriagu, J. O. and Soon, Y. K.: Distribution and isotopic composition of sulfur in lake sediments of northern Ontario. Geochim. Cosmochim. Acta, 49, 823-834, 1985.
Oren, A.: Bioenergetic aspects of halophilism. Microbiol. Mol. Biol. Rev., 63, 334-348, 1999.

Overmann, J., Beatty, J. T., Krouse, H. R. and Hall, K. J.: The sulfur cycle in the chemocline of a meromictic salt lake. Limnol. Oceanogr., 41, 147-156, 1996.

Owens, J. D., Gill, B. C., Jenkyns, H. C., Bates, S. M., Severmann, S., Kuypers, M. M. M., Woodfine, R. G. and Lyons, T. W.: Sulfur isotopes track the global extent and dynamics of euxinia during Cretaceous Oceanic Anoxic Event 2. Proc. Nat. Acad. Sci. (U.S.A.), 110, 18407-18412, 2013.

Paytan, A., Kastner, M., Campbell, D. and Thiemens, M. H.: Sulfur isotopic composition of Cenozoic seawater sulfate. Science, 282, 1459-1462, 1998.

Paytan, A., Kastner, M., Campbell, D. and Thiemens, M. H.: Seawater sulfur isotope fluctuations in the Cretaceous. Science, 304, 1663-1665, 2004.

Peterson, B. J. and Howarth, R. W.: Sulfur, carbon, and nitrogen isotopes used to trace organic matter flow in the salt-march estuaries of Sapelo Island, Georgia. Limnol. Oceanogr., 32, 1195-1213, 1987.

Planavsky, N. J., Bekker, A., Hofmann, A., Owens, J. D. and Lyons, T. W.: Sulfur record of rising and falling marine oxygen and sulfate levels during the Lomagundi event. Proc. Nat. Acad. Sci. (U.S.A.), 109, 18300-18305, 2012.

Price, F. T. and Casagrande, D. J.: Sulfur distribution and isotopic composition in peats from the Okefenokee Swamp, Georgia and the Everglades, Florida. Internat. J. Coal Geol., 17, 1-20, 1991.

Purdy, K., Hawes, I., Bryant, C. L., Fallick, A. E. and Nedwell, D. B.: Estimates of sulphate reduction rates in Lake Vanda, Antarctica support the proposed recent history of the lake. Antarct. Sci., 13, 393, 2001.

Rees, C.E.: ~~, 1973.~~ A steady-state model for sulphur isotope fractionation in bacterial reduction processes. Geochim. Cosmochim. Acta 27, 1141-1162, 1973.

Rickard, D. T.: Kinetics and mechanism of pyrite formation at low temperatures. Am. J. Sci., 275(6), 636-652, 1975.

Ries, J. B., Fike, D. A., Pratt, L. M., Lyons, T. W. and Grotzinger, J. P.: Superheavy pyrite ($\delta^{34}S_{pyr}>\delta^{34}S_{CAS}$) in the terminal Proterozoic Nama Group, southern Namibia: a consequence of low seawater sulfate at the dawn of life. Geology, 37, 743-746, 2009.

Röhl, H.-J., Schmid-Röhl, A., Oschmann, W., Frimmel, A. and Schwark, L.: The Posidonia Shale (Lower Toarcian) of SW-Germany: an oxygen-depleted ecosystem controlled by sea level and palaeoclimate. Palaeogeogr. Palaeoclimatol. Palaeoecol. 165, 27-52, 2001.

Rudnicki, M. D., Elderfield, H. and Spiro, B.: Fractionation of sulfur isotopes during bacterial sulfate reduction in deep ocean sediments at elevated temperatures. Geochim. Cosmochim. Acta, 65(5), 777–789, 2001.

Scheiderich, K., Zerkle, A. L., Helz, G. R., Farquhar, J. and Walker, R. J.: Molybdenum isotope, multiple sulfur isotope, and redox-sensitive element behavior in early Pleistocene Mediterranean sapropels. Chem. Geol., 279, 134-144, 2010.

Shen, Y. A., Buick, R. and Canfield, D. E.: Isotopic evidence for microbial sulphate reduction in the early Archaean era. Nature, 410, 77-81, 2001.

Sim, M. S., Bosak, T. and Ono, S. H.: Large sulfur isotope fractionation does not require disproportionation. Science, 333, 74-78, 2011a.

Formatted: Font: (Default) Calibri, Do not check spelling or grammar

Formatted: Font: (Default) Calibri, Do not check spelling or grammar

Formatted: Font: (Default) Calibri, Not Italic, Do not check spelling or grammar

Formatted: Font: (Default) Calibri, Not Italic, Do not check spelling or grammar

Formatted: Indent: Left: 0", Hanging: 0.5"

Formatted: Font: (Default) Calibri, Do not check spelling or grammar

Formatted: Font: (Default) Calibri, Do not check spelling or grammar

Formatted: Indent: Left: 0", Hanging: 0.5", Space Before: 0 pt, After: 0 pt, Adjust space between Latin and Asian text, Adjust space between Asian text and numbers

Sim, M. S., Ono, S. H., Donovan, K., Templer, S. P. and Bosak, T.: Effect of electron donors on the fractionation of sulfur isotopes by a marine *Desulfovibrio* sp. Geochim. Cosmochim. Acta, 75, 4244-4259, 2011b.
Song, H. Y., Tong, J., Algeo, T. J., Song, H. J., Qiu, H., Zhu, Y., Tian, L., Bates, S., Lyons, T. W., Luo, G. M. and Kump, L. R.: Early Triassic seawater sulfate drawdown. Geochim. Cosmochim. Acta, 128, 95-113, 2014.
Sørensen, K. B. and Canfield, D. E.: Annual fluctuations in sulfur isotope fractionation in the water column of a euxinic marine basin. Geochim. Cosmochim. Acta, 68, 503-515, 2004.
Stam, M. C., Mason, P. R. D., Pallud, C. and Van Cappellen, P.: Sulfate reducing activity and sulfur isotope fractionation by natural microbial communities in sediments of a hypersaline soda lake (Mono Lake, California). Chem. Geol., 278, 23-30, 2010.
Sternbeck, J. and Sohlenius, G.: Authigenic sulfide and carbonate mineral formation in Holocene sediments of the Baltic Sea. Chem. Geol., 135, 55-73, 1997.
Strauss, H.: The isotopic composition of sedimentary sulfur through time. Palaeogeogr. Palaeoclimatol. Palaeoecol. 132, 97-118, 1997.
Strauss, H.: Geological evolution from isotope proxy signals—sulfur. Chem. Geol., 161, 89-101, 1999.
Strauss, H.: Sulfur isotopes and the early Archaean sulphur cycle. Precambr. Res., 126, 349-361, 2003.
Stribling, J. M., Cornwell, J. C. and Currin, C.: Variability of stable sulfur isotopic ratios in *Spartina alterniflora*. Mar. Ecol. Progr. Ser., 166, 73-81, 1998.
Suits, N. S. and Wilkin, R. T.: Pyrite formation in the water column and sediments of a meromictic lake. Geology, 26, 1099-1102, 1998.
Sweeney, R. E. and Kaplan, I. R.: Stable isotope composition of dissolved sulfate and hydrogen sulfide in the Black Sea. Mar. Chem., 9, 145-152, 1980.
Valentine, D. L.: Biogeochemistry and microbial ecology of methane oxidation in anoxic environments: a review. Antonie van Leeuwenhoek, 81, 271-282, 2002.
Wacey, D., McLoughlin, N., Whitehouse, M. J. and Kilburn, M. R.: Two coexisting sulfur metabolisms in a ca. 3400 Ma sandstone. Geology, 38, 1115-1118, 2010.
Werne, J. P., Hollander, D. J., Behrens, A., Schaeffer, P., Albrecht, P. and Damsté, J. S. S.: Timing of early diagenetic sulfurization of organic matter: A precursor-product relationship in Holocene sediments of the anoxic Cariaco Basin, Venezuela. Geochim. Cosmochim. Acta, 64, 1741-1751, 2000.
Werne, J. P., Lyons, T. W., Hollander, D. J., Formolo, M. J. and Damsté, J. S. S.: Reduced sulfur in euxinic sediments of the Cariaco Basin: sulfur isotope constraints on organic sulfur formation. Chem. Geol., 195, 159-179, 2003.
Werne, J. P., Lyons, T. W., Hollander, D. J., Schouten, S., Hopmans, E. C. and Damsté, J. S. S.: Investigating pathways of diagenetic organic matter sulfurization using compound-specific sulfur isotope analysis. Geochim. Cosmochim. Acta, 72, 3489-3502, 2008.
Wijsman, J. W. M., Middelburg, J. J., Herman, P. M. J., Böttcher, M. E. and Heip, C. H. R.: Sulfur and iron speciation in surface sediments along the northwestern margin of the Black Sea. Mar. Chem., 74, 261-278, 2001.

Formatted: Indent: Left: 0", Hanging: 0.5", Space Before: 0 pt, After: 0 pt, Adjust space between Latin and Asian text, Adjust space between Asian text and numbers

Wilkin, R. T., Barnes, H .L. and Brantley, S.L.: The size distribution of framboidal pyrite in marine sediments: an indicator of redox conditions. Geochim. Cosmochim. Acta, 60, 3897-3912, 1996.

Wortmann, U. G. and Chernyavsky, B. M.: Effect of evaporite deposition on Early Cretaceous carbon and sulphur cycling. Nature, 446, 654-656, 2007.

Wortmann, U. G. and Paytan, A.: Rapid variability of seawater chemistry over the past 130 million years. Science, 337, 334-336, 2012.

Wortmann, U. G., Bernasconi, S. M. and Böttcher, M. E.: Hypersulfidic deep biosphere indicates extreme sulfur isotope fractionation during single-step microbial sulfate reduction. Geology, 29, 647-650, 2001.

Wotte, T., Strauss, H., Fugmann, A. and Garbe-Schönberg, D.: Paired $\delta^{34}S$ data from carbonate-associated sulfate and chromium-reducible sulfur across the traditional Lower-Middle Cambrian boundary of W-Gondwana. Geochim. Cosmochim. Acta, 85, 228-253, 2012.

Wu, N., Farquhar, J., Strauss, H., Kim, S.-T. and Canfield, D. E.: Evaluating the S-isotope fractionation associated with Phanerozoic pyrite burial. Geochim. Cosmochim. Acta, 74, 2053-2071, 2010.

Zaback, D. A. and Pratt, L. M.: Isotopic composition and speciation of sulfur in the Miocene Monterey Formation: Reevaluation of sulfur reactions during early diagenesis in marine environments. Geochim. Cosmochim. Acta, 56, 763-774, 1992.

Zerkle, A. L., Kamyshny, A., Jr., Kump, L. R., Farquhar, J., Oduro, H. and Arthur, M. A.: Sulfur cycling in a stratified euxinic lake with moderately high sulfate: Constraints from quadrupole S isotopes. Geochim. Cosmochim. Acta, 74, 4953-4970, 2010.

Zhang, S., Jiang, G., Zhang, J., Song, B., Kennedy, M. J. and Christie-Blick, N.: U-Pb sensitive high-resolution ion microprobe ages from the Doushantuo Formation in south China: constraints on late Neoproterozoic glaciations. Geology, 33, 473-476, 2005.

Zhang, S., Jiang, G. and Han, Y.: The age of the Nantuo Formation and Nantuo glaciation in South China. Terra Nova, 20, 289-294, 2008.

Figure captions

Fig. 1. The rate method. On a crossplot of a~~A~~queous sulfate concentration~~s~~ ($[SO_4^{2-}]_{aq}$) versus S-isotopic fractionation between cogenetic sulfate and sulfide ($\Delta^{34}S_{sulfate\text{-}sulfide}$), ~~. T~~the diagonal blue lines represent maximum rates of change in sulfate $\delta^{34}S$ (i.e., $\partial\delta^{34}S_{SO4}/\partial t(max)$). For paleomarine systems, maximum seawater sulfate concentrations ($[SO_4^{2-}]_{SW}$(max))) can be estimated from the abscissa based on measured values of $\Delta^{34}S_{CAS\text{-}PY}$ and $\partial\delta^{34}S_{CAS}/\partial t(max)$. The two scales on the abscissa represent $[SO_4^{2-}]_{SW}$ in oxic (O) and anoxic (A) oceans, in which pyrite burial fluxes are equal to 4×10^{13} g yr^{-1} and 10×10^{13} g yr^{-1} (i.e., 40% and 100% of the modern total sulfur~~S~~ sink flux), respectively. The typical range of $\Delta^{34}S_{sulfate\text{-}sulfide}$ due to MSR fractionation in modern ~~seawater~~ marine systems is 30-60‰ (Habicht and Canfield, 1997). The maximum rate of seawater sulfate $\delta^{34}S$ variation during the Cenozoic is ~0.~~5~~7‰ Myr^{-1} (Paytan et al., 1998), yielding estimates of ~40-80~~110~~ mM for $[SO_4^{2-}]_{SW}$ through projection to the abscissa (dashed lines). These estimates exceed actual modern seawater $[SO_4^{2-}]$, which is ~29 mM (Millero, 2005) because the ~~*observed*~~ *measured* maximum rate of $\partial\delta^{34}S_{SO4}/\partial t$ (light blue parallelogram) is less than the *theoretical* possible maximum rate (~1-2‰ Myr^{-1}; red parallelogram).

Fig. 2. The MSR-trend method. ~~Aqueous sulfate concentration ($[SO_4^{2-}]_{aq}$) versus S-isotopic fractionation between aqueous sulfate and aqueous or sedimentary sulfide ($\Delta^{34}S_{sulfate\text{-}sulfide}$).~~ **(a)** Data from 81 modern aqueous systems (Table A1). The non-hypersaline environments (n = 75) yield a linear regression (solid line; y = 0.42x ~~– 0.15~~+ 1.10 in log units) ~~with~~ having r^2 = ~~+~~0.9~~8~~0 (t-statistic = 1.99, ($p(\alpha)$ <0.01) and a limited ~~a narrow regression line~~ uncertainty range (dashed lines). ~~F_{MSR} is~~The MSR trend thus ~~a~~ represents a process with an order of reaction (n) of 0.42 and a rate constant (k) ~~of -0.15~~of 1.10 (cf. Jones et al., 2007). The gray field encloses most of the data from Table A1 and highlights the overall trend. A~~Separate~~ ~~a~~nalysis of the dataset by redox environment yielded statistically indistinguishable trends for oxic (y = 0.48x + 1.10~~-0.26~~; r^2 = ~~+~~0.~~77~~88, n = 44, $p(\alpha)$ <0.01) and euxinic settings (y = 0.40x + 1.06~~-0.08~~; r^2 = ~~+~~0.8~~90~~, n = 31, $p(\alpha)$ <0.01). The Habicht et al. (2002) dataset of 60 sulfate-reducing microbial (SRM) ~~experimental determinations of MSR~~culture values is shown for comparison; these data have been converted ~~from their original log-linear~~ to log-log format, and data points that are off scale (i.e., ~~with~~ $\Delta^{34}S_{sulfate\text{-}sulfide}$ <1‰) are shown by triangles on the abscissa. Neither the ~~6~~ six hypersaline environments in our dataset (red symbols) nor the Habicht et al. data (small open circles) were included in the regression analysis. **(b)** Use of the MSR trend to estimate paleo-~~ancient~~ seawater $[SO_4^{2-}]_{aq}$. Measured values of $\Delta^{34}S_{sulfate\text{-}sulfide}$ are projected from the ordinal scale to the MSR trend and then to the abscissa. Note that uncertainty in the slope of the MSR trend is ~~taken into consideration~~accommodated by projection to the upper uncertainty limit for $\Delta^{34}S_{sulfate\text{-}sulfide}$ maxima and to the lower uncertainty limit for $\Delta^{34}S_{sulfate\text{-}sulfide}$ minima. The vertical black bar at $[SO_4^{2-}]_{aq}$ = ~~4~~1.45 (i.e., the modern seawater sulfate concentration of 29 mM) represents the range of F_{MSR} variation among modern marine SRM~~microbial~~ communities.

Formatted: Font: Italic

Formatted: Font: Symbol

Fig. 3. (a) Phanerozoic seawater sulfate $\delta^{34}S$. Data sources: Cenozoic (Paytan et al., 1998; red circles), Cretaceous (Paytan et al., 2004; black squares), and pre-Cretaceous (Kampschulte and Strauss, 2004; blue triangles; Table A2). SAverage secular variation in $\delta^{34}S_{SO4\text{-}SW}$ is shown by a mean LOWESS means curve (blue line for calculations at low-resolution (5-Myr) steps; and red line for high-resolution (1-Myr steps) records) and a standard deviation (±1σ) standard deviation range (green field for 5-Myr steps low-resolution record; Table A3). Pre-Cretaceous and Cretaceous-Cenozoic estimates of $\delta^{34}S_{SO4\text{-}SW}$ have uncertainties of ±2-7‰ and ±<1‰, respectively. The lThe labels represent four short-term (<2-Myr) intervals of known high-frequency $\partial\delta^{34}S_{SO4}/\partial t$ variation (EMCB = Early-Middle Cambrian boundary; SPICE = Steptoean positive carbon isotope excursion; see text for discussion; CTB = Cenomanian-Turonian boundary). **(b)** Rate of seawater $\delta^{34}S$ variation ($\partial\delta^{34}S_{SO4}/\partial t$), as calculated from the seawater sulfate $\delta^{34}S$ LOWESS curves. The maximum Phanerozoic $\partial\delta^{34}S_{SO4}/\partial t$ is <4‰ Myr^{-1}, although rates of 10 to >50‰ Myr^{-1} have been reported from some high-resolution CAS studies. **(c)** $\Delta^{34}S_{CAS\text{-}PY}$ for Phanerozoic marine sediments. D(data from figure 3 of Wu et al., (2010). The continental glaciation record is adapted from Montañez et al. (2011); all ages were converted to the Gradstein et al. (2012) timescale.

Fig. 4. Phanerozoic seawater $[SO_4^{2-}]$ (Table A3). The MSR-trend method (Eqs. 6-8) yields an estimate of mean $[SO_4^{2-}]_{SW}$ (blue curve; bracketed by a ±1σ s.d. band). The rate method (Eqs. 3-4) yields the maximum possible $[SO_4^{2-}]_{SW}$; the black and red curves show maximum values based on the low- and high-frequency Phanerozoic $\delta^{34}S_{CAS}$ records, respectively (Fig. ure 3a), and the dashed red line represents the lower envelope of the high-frequency curve. The modern seawater $[SO_4^{2-}]$ of ~29 mM is shown by the red arrow.

Fig. 5. Comparison of Phanerozoic seawater sulfate $[SO_4^{2-}]$ records. The mean trend of the present study is shown by a heavy blue line, with the ±1σ uncertainty range shown as a blue band. Estimates are based either on fluid-inclusion studies (Horita et al., 2002; Brennan et al., 2004; Lowenstein et al., 2005) or C-S-cycle modeling (Holser et al., 1989; Berner, 2004; Gill et al., 2007; Wortmann and Chernyavsky, 2007; Wortmann and Paytan, 2012; Halevy et al., 2012). Arrows indicate unconstrained minimum or maximum values.

Fig. 6. Analysis of seawater sulfate concentrations for 10 late Neoproterozoic marine units. The parallelogram for each unit was generated using the rate method. A summary of results and dData sources are is given in Table A4; other details as in Figures 1-2.

Fig. 7. Analysis of seawater sulfate concentrations for 8 Paleozoic marine units. The parallelogram for each unit was generated using the rate method. The red field represents the long-term average $\Delta^{34}S_{CAS\text{-}PY}$ for the Paleozoic based on data in Wu et al. (2010). Data A summary of results and data sources are is given in Table A4; other details as in Figures 1-2.

Fig. 8. Analysis of seawater sulfate concentrations for 8 Mesozoic-Cenozoic marine units. The parallelogram for each unit was generated using the rate method. The red field represents the long-term average $\Delta^{34}S_{CAS\text{-}PY}$ for the Mesozoic-Cenozoic based on data in Wu et al.

(2010). A summary of results and d~~D~~ata sources ~~are~~ is given in Table A4; other details as in Figures 1-2.

Fig. 9. Interpretation of deviations ~~of rate-based~~in $[SO_4^{2-}]_{SW}$ estimates ~~from~~ between the rate and MSR-trend ~~-based $[SO_4^{2-}]$ estimates~~ methods. Type ~~1~~ I deviations, in which rate ~~-based~~ method estimates are anomalously high (lower right field), are likely to reflect extremely stable environmental conditions, in which the marine sulfur cycle is in equilibrium (i.e., balanced source and sink fluxes). Type ~~2~~ II deviations, in which rate-based estimates are anomalously low (upper left field), are likely to reflect sulfate reduction in semi-restricted ~~-~~ marine basins. In this case, $\Delta^{34}S_{CAS\text{-}PY}$ will be controlled by $[SO_4^{2-}]_{SW}$, which may be equal or close to that of the global ocean, but $\partial\delta^{34}S_{CAS}/\partial t(max)$ will be controlled by the mass of aqueous sulfate within the restricted basin, which will be a function of basin volume.

Fig. 10. Seawater sulfate concentrations for late Neoproterozoic and Phanerozoic marine units (Figs. 6-8) compared with long-term $[SO_4^{2-}]_{SW}$ curve (Fig. 4). Estimates of $[SO_4^{2-}]_{SW}$ are based on (1) the rate method (calculated per Eqs. 3-4; shown as open boxes) and (2) the MSR-trend method (calculated per Eqs. 6-8; shown as ~~colored~~ solid boxes); note that unit symbols and colors are keyed to Table A4 and Figures 6-8. See text for discussion. Other details as in Figure 4.

Formatted: Subscript